BIODIVERSITAS
Volume 25, Number 12, December 2024
Pages: 4642-4663

ISSN: 1412-033X
E-ISSN: 2085-4722
DOI: 10.13057/biodiv/d251202

Diversity of epilithic diatoms from coral reef ecosystem of Bawean Island, Indonesia

OKTIYAS MUZAKY LUTHFI[1,2,♥], YENNY RISJANI[2,3], NAGARAJ SUBRAMANI[4], MATEUSZ RYBAK[5], JINSOON PARK[6], MAŁGORZATA BĄK[1], ANDRZEJ WITKOWSKI[1]

[1]Institute of Marine and Environmental Sciences, University of Szczecin. ul. Mickiewicza 16, 70-383 Szczecin, Poland
[2]Faculty of Fisheries and Marine Sciences, Universitas Brawijaya. Jl. Veteran, Malang 65145, East Java, Indonesia. Tel.: +62-341-553512, Fax.: +62-341-557837, ♥email: omuzakyl@ub.ac.id
[3]Center for Algae and Environment, (ALGAEN) LPPM, Universitas Brawijaya. Jl. Veteran, Malang 65145, East Java, Indonesia
[4]Centre for Advanced Studies in Botany, University of Madras. Guindy Campus, Chennai, Tamil Nadu 600025, India
[5]College of Natural Sciences, University of Rzeszów. ul. Zelwerowicza 4, 35-601, Rzeszów, Poland
[6]School of Earth and Environmental Sciences (Oceanography), Seoul National University. 1 Gwanak-ro, Gwanak-gu, Seoul 08826, Republic of Korea

Manuscript received: 11 October 2024. Revision accepted: 1 December 2024.

Abstract. *Luthfi OM, Risjani Y, Subramani N, Rybak M, Park J, Bąk M, Witkowski A. 2024. Diversity of epilithic diatoms from coral reef ecosystem of Bawean Island, Indonesia. Biodiversitas 25: 4642-4663.* This study investigates the diversity and community structure of epilithic diatoms in the coral reef ecosystems of Bawean Island, Indonesia. A total of 137 taxa from 49 genera were identified from coral rubble habitats across four distinct locations. The Shannon-Wiener Diversity Index (H') and Dominance Index (C) were used to assess species diversity and dominance, revealing that Station 4 exhibited the highest diversity (H' = 3.88) and lowest dominance (C = 0.03), while Station 2 had the lowest diversity (H' = 2.55) and highest dominance (C = 0.09). Evenness values (E = 0.9) were consistent across all sites, indicating a uniform distribution of species. The findings suggest that coral rubble provides unique microhabitats conducive to diatom diversity, challenging the conventional understanding that habitat diversity correlates positively with species diversity. The study also compares Bawean Island's diatom diversity with other regions, noting its intermediate diversity level, which may be influenced by its geographical position between Kalimantan and Java. The presence of dominant species like *Diploneis crabro*, *Petroneis marina*, *Halamphora coffeiformis,* and *Trachyneis aspera* underscores the ecological significance of these diatoms in coral reef ecosystems. This research fills a significant gap in our understanding of the marine biodiversity and ecological dynamics of Bawean Island, highlighting the importance of diatoms in maintaining the health and stability of coral reef ecosystems and its potential implications for future research and conservation efforts.

Keywords: Biodiversity, coral reef ecosystems, microhabitats, Shannon-Wiener Index, volcanic island

Abbreviations: C: *Catenula*; Ca: *Catenulopsis*

INTRODUCTION

The Indonesian archipelago's vast coral reef system, spanning 51,000 square kilometers (Done 2011), represents one of nature's most remarkable laboratories for studying marine biodiversity and ecological interactions. Within this complex ecosystem, our research has revealed intricate relationships between coral communities and microscopic diatoms that contribute fundamentally to reef health and stability. The positioning of Indonesia within the Coral Triangle has provided us with unprecedented opportunities to study these interactions across diverse reef environments, from fringing reefs to extensive barrier systems, supporting approximately 574 coral species, representing 72% of the world's total (Madduppa et al. 2021). The structural complexity of coral reefs offers shelter and breeding grounds for many marine organisms, contributing significantly to the overall biodiversity of the ocean; for instance, the Great Barrier Reef in Australia is home to over 1,500 species of fish and 4,000 species of mollusks (Glynn and Enochs 2010; Claudino-Sales 2019). These reefs are further reinforced by other calcareous biota, including coralline algae and mollusks, which contribute additional calcium carbonate, enhancing the reef's resilience and stability. Diatoms, a type of microalgae, play a crucial role in the reef ecosystem by contributing to primary production and forming the basis of the food web. Diatom frustules are made of silica; once diatoms die, their silica-rich frustules accumulate and integrate into the reef matrix, providing additional strength and stability. This process not only supports the physical framework of the reef but also fosters a more resilient ecosystem capable of withstanding environmental stressors.

The interaction between marine diatoms with coral reefs in a direct way is unclear. However, as microscopic algae, diatoms play a crucial role in the health and productivity of coral reef ecosystems. They contribute significantly to the primary production within coral reefs, serving as a vital food source for various marine organisms in reef ecosystems, enhancing nutrient cycling, and promoting coral growth through the provision of essential nutrients (Lobban et al. 2012). Marine diatoms mostly occur in various substrates of the reef, such as colonizing sand, macroalgae (*Halimeda*, *Padina*, *Sargassum*), marine plants (seagrass), dead coral, coral rubble, and very view reported from life coral (Car et al. 2019; Majewska and Van de Vijver 2020; Luthfi et al. 2023). Coral rubble in Bawean is commonly found in reef flat areas and accumulates with algae, forming a band or rampart. Coral rubble is fragmented dead coral due to biology and mechanical processes in nature (Wolfe et al. 2021). Despite coral rubble creating unstable substrates, they create microhabitats that support a diverse assemblage of marine life, from small invertebrates (coral juveniles, sponges) and diatoms to juvenile fish, enhancing the overall biodiversity of the reef.

Coral reefs in Bawean Island, Indonesia form a fringing reef near the shore and patch reef offshore. Offshore patch reefs in Bawean waters occur as isolated reef structures, rising from deeper sandy substrates and reaching depths of 3-10 meters below the surface (Luthfi and Anugrah 2017). These patch reefs, while smaller in extent compared to the fringing reefs, often demonstrate higher coral cover percentages and species diversity, potentially due to reduced coastal influences and sedimentation impacts. Despite the rich biodiversity of Bawean Island's marine ecosystems, there has been a notable absence of research specifically focused on epilithic diatoms in this region. Epilithic diatoms, which grow on hard substrates such as rocks and coral rubble surfaces, play a crucial role in primary production and nutrient cycling within coral reef ecosystems. The lack of studies on these diatoms on Bawean Island represents a significant gap in our understanding of the island's marine biodiversity and ecological dynamics. The objectives of this research are to assess the diversity and distribution of epilithic diatoms on Bawean Island and to understand the ecological roles of these diatoms in coral reef ecosystems.

MATERIALS AND METHODS

Study area and diatom samplings

Diatom samplings

On 7 January 2021, diatom samples were collected from four distinct locations on Bawean Island in the Java Sea, Gresik District, East Java Province, Indonesia, i.e.: Gili Iyang Harbour, *Mangrove Hijau Daun* - MHD, Mombhul, and Selayar Beach. These sites, detailed in Table 1 and illustrated in Figure 1, were chosen for their representative reef flat areas. The diatom samples were specifically obtained from coral rubble, which consists of fragments of dead coral.

Light microscopy

Diatom samples were carefully scraped from coral rubble using a toothbrush and collected in 50 ml Falcon bottles. To remove carbonate minerals, the samples were treated with 10% hydrochloric acid (HCl) for two days. Following this acid treatment, the samples underwent three thorough washes with distilled water to eliminate any residual acid. Subsequently, to remove organic matter, the samples were treated with 37% hydrogen peroxide (H_2O_2) and boiled for 4-5 hours. This boiling process ensures the complete oxidation of organic materials. Finally, the samples were washed five times with distilled water to ensure the removal of any remaining chemicals. A water suspension of the cleaned diatom samples was pipetted onto coverslips and left at room temperature for 24 hours to allow the water to evaporate (Kryk et al. 2021).

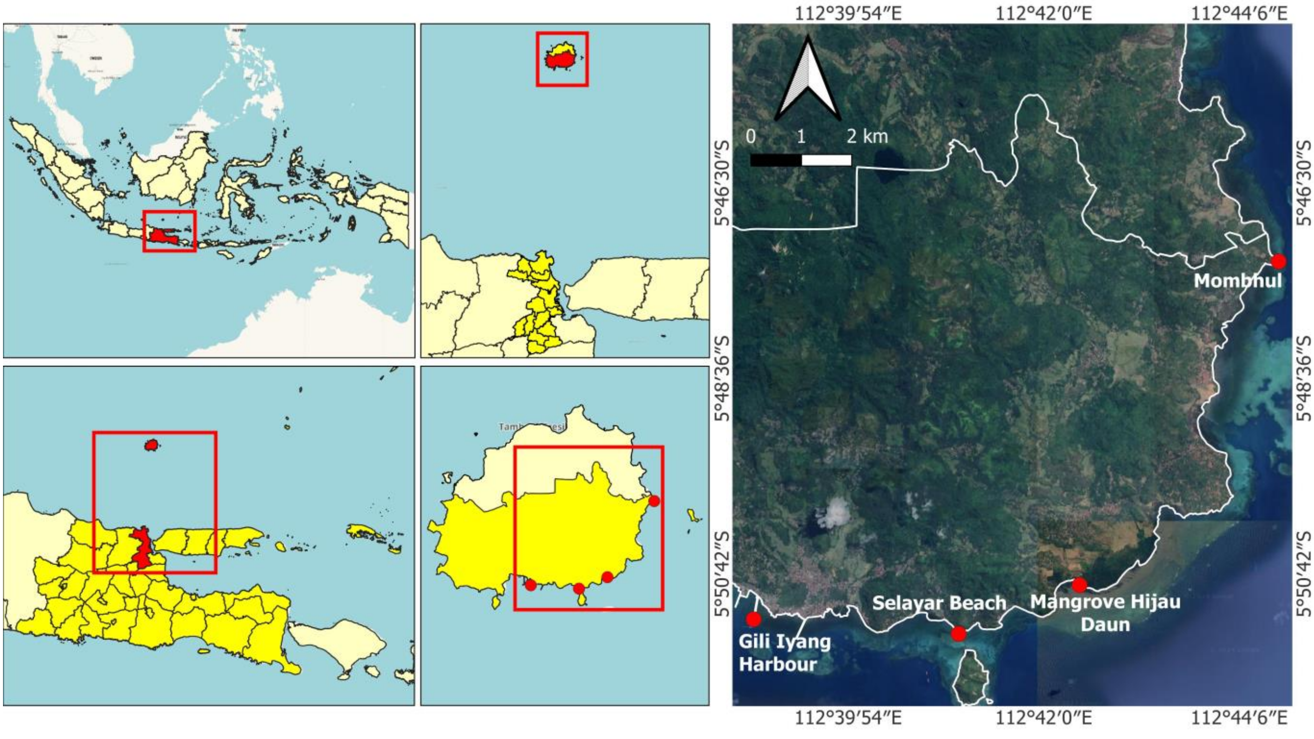

Figure 1. Sampling sites are indicated by red dots, in Bawean Island, Gresik District, East Java Province, Indonesia

Once dry, the coverslips were mounted onto glass slides using Naphrax®. Light Microscopic (LM) micrographs were then taken using a Zeiss Axio Scope A1 light microscope (Carl Zeiss, Jena, Germany). The microscope was equipped with a 100× Plan Apochromatic oil immersion objective and a Canon EOS 500D camera, ensuring high-resolution imaging of the diatom frustules. Undamaged frustules/valves were enumerated in the datasheet following the method described by Hasle and Fryxell (1970).

Biodiversity, Dominance, and Evenness Indices

To assess the diatom community structure, we calculated three ecological indices: Shannon-Wiener Diversity Index (H'), Simpson's Dominance Index (C), and Pielou's Evenness Index (E). The Shannon-Wiener Index was computed to measure species diversity, accounting for both abundance and evenness of the species present. It is calculated by summing the product of the proportion of each species and the natural logarithm of that proportion, then multiplying the result by -1 (Shannon 1948). Simpson's dominance index was used to quantify the concentration of dominance within the community, calculated as the sum of the squared proportions of each species (Magurran 1988, 2003). Pielou's evenness index was calculated to represent how evenly the individuals were distributed among the different species. It is derived by dividing the Shannon-Wiener index by the natural logarithm of the total number of species (Pielou 1966). Relative abundance was calculated as the percentage of each species or taxon about the total number of identified species from all stations. Dominant species were defined as those comprising more than 1% of the total valve count in any given sample (Risjani et al. 2021). Furthermore, to determine the significance of diversity among stations, a one-way Analysis of Variance (ANOVA) was performed using MS. Excell software.

RESULTS AND DISCUSSION

Diatom classification

The diatom taxa are systematically categorized according to the framework established by Ruggiero et al. (2015).

Phylum	**:**	Ochrophyta Cavalier-Smith
Class	**:**	Bacillariophyceae Haeckel
Sub-class	**:**	Coscinodiscophycidae Round & R.M.Crawford
		Fragilariophycidae Round
		Bacillariophycidae D.G. Mann

Sub-class: Coscinodiscophycidae
Order: Coscinodiscales

Actinocyclus subtilis (W.Gregory) Ralfs, 1861 (Figure 2E). **References:** Witkowski et al. (2000), pages 450-451, pl. 4, Figure 1; López-Fuerte et al. (2020) page 39, Figures 9 (A-E). **Dimensions:** Diameter 31.9 µm, areolae in valve center 24 in 10 µm.

Order: Melosirales

Hyalodiscus scoticus (Kützing) Grunow, 1879 (Figure 2A). **References:** Witkowski et al. (2000), pages 456-457, pl. 7, Figures 3, 4. **Dimensions:** Diameter 41.9 µm, areolae in valve center 20 in 10 µm, areolae on valve margin 20 in 10 µm.

Order: Paraliales

Paralia sulcata (Ehrenberg) Cleve, 1873 (Figures 2.F-2.I). **References:** López-Fuerte et al. (2020), page 40, Figures 10 (G-L). **Dimensions:** Diameter 9.4-31.5 µm, areolae on valve margin 18-20 in 10 µm. **Comment:** Figure 2 (H) in different focal length plane

Order: Thalassiosirales

Thalassiosira sp. (Figures 2.C, 2.D). **References:** López-Fuerte et al. (2010), pages 111-112, Figures 5-8. **Dimensions:** Diameter 16-21.5 µm, areolae in valve center 10-12 in 10 µm, fultoportulae 5 in 10 µm. **Comments:** The specimen is similar to *Thalassiosira oestrupii* (Ostenfeld) Hasle with denser areolae

Order: Triceratiales

Plagiogramma cf. *pulchellum* Greville, 1859 var. *pymae* (Figure 2.Q). **References:** Foged (1975), pages 80-81, pl. VIII, Figures 1, 2. **Dimensions:** Length 25.6 µm, width 9.5 µm, striae 18 in 10 µm, areolae 20 in 10 µm. **Comment:** The described specimen has distinctively finer striae and areolae compared to the original report.

Plagiogramma rhombicum Hustedt, 1955 (Figure 2.R). **References:** Witkowski et al. (2000), pages 464-465, pl. 11, Figure 33. **Dimensions:** Length 23.7 µm, width 6.9 µm, striae 10 in 10 µm.

Plagiogramma staurophorum (W.Gregory) Heiberg, 1863 (Figure 2.P). **References:** Witkowski et al. (2000), pages 464-465, pl. 11, Figures 16-21. **Dimensions:** Length 33.1 µm, width 13.6 µm, striae 8 in 10 µm, areolae 8 in 10 µm.

Sub-class: Fragilariophycidae
Order: Ardissoneales

Ardissonea robusta (Ralfs ex Pritchard) De Notaris, 1871 (Figure 3.A). **References:** Beltrones et al. (2021), page 15, Figure 9 (D,E). **Dimensions:** Length 205.2 µm, width 13.9 µm, striae 10 in 10 µm, areola 28 in 10 µm. **Comment:** Basionym *Synedra robusta* Ralfs.

Order: Licmophorales

Trachysphenia sp. (Figure 2.J). **Dimensions:** Length 24.3 µm, width 4.6 µm, striae 12 in 10 µm, areola 20 in 10 µm. **Comments:** Valve outline similar to *Licmophora abbreviata*, which is not areolate in its striae

Tabularia fasciculata (C.Agardh) D.M.Williams & Round, 1986 (Figure 2.O). **References:** Beltrones et al. (2021), page 15, Figure 9 (j). **Dimensions:** Length 48.9 µm, width 26 µm.

Grammatophora angulosa var. *islandica* (Ehrenberg) Grunow, 1881 (Figure 2.T). **References:** Witkowski et al. (2000), pages 472-473, pl. 15, Figure 6. **Dimensions:** Length 9.7 µm, width 10.7 µm.

Grammatophora marina var. *undata* Cleve-Euler, 1949 (Figure 2.S). **References:** Witkowski et al. (2000), pages 472-473, pl. 15, Figures 9-12; Álvarez-Blanco and Blanco (2014), pages 228-229, pl. 12, Figures 1-12; Foged (1975), pages 78-79, pl. VII, Figure 5. **Dimensions:** Length 20.1 µm, width 10.6 µm.

Order: Rhaphoneidales

Psammodiscus nitidus (W.Gregory) Round & D.G.Mann, 1980 (Figure 2.B). **References:** Navarro (1981), page 429, Figure 22; Lobban et al. (2012), page 258, pl. 14, Figures 6, 7; Al-Handal et al. (2016), page 11, pl. 1, Figure 6; Beltrones et al. (2021), page 54, Figure 3 (E); John (2016), page 173, Figure 74. **Dimensions:** Diameter 38.6 µm, areolae in valve center 5 in 10 µm, areolae on valve margin 10 in 10 µm.

Rhaphoneis cf. *amphiceros* (Ehrenberg) Ehrenberg, 1844 (Figure 2.K). **References:** Foged (1975), pages 82-83, pl. IX, Figure 2. **Dimensions:** Length 25.7 µm, width 17.5 µm, striae 7 in 10 µm, areola 6 in 10 µm. **Comments:** It is different from typical specimens of *Rhaphoneis amphiceros* with its quadrate areolae as well as broad and short apices. It could be a new species.

Sub-class: Bacillariophycidae D.G. Mann

Order: Achnanthales

Amphicocconeis disculoides (Hustedt) Stefano & Marino, 2003 (Figure 3.B). **References:** De Stefano and Marino (2003), page 363, Figures 1-10. **Dimensions:** Length 9.4 µm, width 6 µm, striae 10 in 10 µm, areola 15 in 10 µm. **Comments:** This species has laterally elongated areolae. Basionym: *Cocconeis disculoides*.

Cocconeiopsis (cf.) *regularis* (Hustedt) Witkowski, Lange-Bertalot & Metzeltin (Figure 3.G). **References:** Witkowski et al. (2000), pages 578-579, pl. 68, Figures 5-8. **Dimensions:** Length 17.5 µm, width 11.7 µm, striae 18 in 10 µm, areola 20 in 10 µm.

Cocconeis guttata Hustedt & Aleem, 1951 (Figures 3.I-3.T). **References:** Beltrones et al. (2021), page 20, Figures 14 (A-G). **Dimensions:** Length 13.7-20.7µm, width 9.3-14.6, striae 8-22 in 10 µm, areola 6-10 in 10 µm.

Cocconeis krammeri Lange-Bertalot & Metzeltin, 1996 (Figure 3.H). **References:** Witkowski et al. (2000), pages 510-511, pl. 34, Figures 4, 5. **Dimensions:** Length 24.2 µm, width 13.8 µm, striae 25 in 10 µm.

Cocconeis scutellum Ehrenberg, 1838 (Figure 3.D). **References:** Witkowski et al. (2000), pages 518-519, pl. 38, Figure 11. **Dimensions:** Length 10.8 µm, width 6.9 µm, striae 18 in 10 µm, areola 16 in 10 µm.

Cocconeis sp. (Figure 3.F). **References:** Kryk (2016), page 95, pl. 7, Figure 138. **Dimensions:** Length 15.4 µm, width 9.7 µm, striae 22 in 10 µm, areola 20 in 10 µm.

Cocconeis stauroneiformis (W.Smith) H.Okuno, 1957 (Figure 3.C). **References:** Witkowski et al. (2000), pages 518-519, pl. 38, Figures 19-25. **Dimensions:** Length 10.5 µm, width 6.7 µm, striae 24 in 10 µm, areola 30 in 10 µm.

Planothidium campechianum (Hustedt) Witkowski, Lange-Bertalot, Metzeltin (Figure 3.E). **References:** Witkowski et al. (2000), pages 538-539, pl. 48, Figures 3-9. **Dimensions:** Length 13.1 µm, width 5.2 µm, striae 16 in 10 µm. **Comment:** With its short interstriae compared to *P. lilljerborgei*. *Planothidium campechianum* was also reported from Micronesia (Park et al. 2022).

Order: Bacillariales

Bacillaria paxillifer (Müller) Marsson (Figure 4.F). **References:** Witkowski et al. (2000), pages 866-867, Figures 9-12. **Dimensions:** Length 59.1 µm, width 5.9 µm, fibulae 8 in 10 µm.

Bacillaria socialis (Gregory) Ralfs, 1861 (Figure 4.E). **References:** Witkowski et al. (2000), pages 834-835, pl. 196, Figures 5-7; pages 856-857, pl. 207, Figure 9. **Dimensions:** Length 90.4 µm, width 7.3 µm, fibulae 4 in 10 µm.

Fragilariopsis sp. (Figure 2.N). **References:** Witkowski et al. (2000), pages 786-787, pl. 172, Figures 17, 18. **Dimensions:** Length 36.5 µm, width 6.1 µm, striae 9 in 10 µm.

Hantzschia kaiseri A.Witkowski, H.Lange-Bertalot & D.Metzeltin, 2000 (Figure 4.P). **References:** Witkowski et al. (2000), pages 792-793, pl. 175, Figures 11-15; pages 880-881, pl. 219, Figures 1-5. **Dimensions:** Length 53.4 µm, width 7.4 µm, fibulae 9 in 10 µm, striae 8 in 10 µm. **Comment:** Comparing others as *H. kaiseri*: 43-66 in 10 µm, fibulae 9-10 in 10 µm; *H. pseudomarina* 46-65 in 10 µm, fibulae 10-13 in 10 µm.

Hantzschia virgata (Roper) Grunow, 1880 (Figure 4.O). **References:** Witkowski et al. (2000), pages 794-795, pl. 176, Figures 1-3; John (2016), pages 404-405, Figure 128 L. **Dimensions:** Length 84.3 µm, width 9.3 µm, fibulae 5 in 10 µm, striae 12 in 10 µm, areola 16 in 10 µm.

Nitzschia cf. *coarctata* Grunow, 1880 (Figure 5.H). **References:** Witkowski et al. (2000), pages 808-809, pl. 183, Figure 13; pages 814-815, pl. 186, Figures 4-13. **Dimensions:** Length 36.8 µm, width 7.5 µm, fibulae 17 in 10 µm, striae 16 in 10 µm, areolae 20 in 10 µm. **Comment:** Similar to *N. ligowskii* has a very wide sternum interrupting the transapical striae. This sternum would be seen as hyaline depressions under LM.

Nitzschia distans var. *tumescens* Grunow, 1880 (Figure 13.G). **References:** Witkowski et al. (2000), pages 848-849, pl. 203, Figure 10. **Dimensions:** Length 32.2 µm, width 3.6 µm, areolae 16 in 10 µm. **Comments:** Girdle view plane.

Nitzschia distans W.Gregory, 1857 (Figure 4.L). **References:** Witkowski et al. (2000), pages 848-849, pl. 203, Figure 7. **Dimensions:** Length 48.6 µm, width 4.8 µm, fibulae 11 in 10 µm.

Nitzschia filiformis Hajós, 1959 (Figures 4.G-4.I). **References:** Witkowski et al. (2000), pages 842-843, pl. 200, Figures 3-8. **Dimensions:** Length 59.1-67.6 µm, width 6.1-6.4 µm, fibulae 7-8 in 10 µm, striae 32-34 in 10 µm.

Nitzschia liebethruthii Rabenhorst, 1864 (Figure 4.K). **References:** Krammer and Lange-Bertalot (1988), pages 354-355, pl. 69, Figures 22-32. **Dimensions:** Length 13.2 µm, width 2.4 µm, fibulae 15 in 10 µm, striae 26 in 10 µm.

Nitzschia scalpelliformis Grunow, 1880 (Figures 4.A-4.D). **References:** Witkowski et al. (2000), pages 844-845, pl. 201, Figures 10-12. **Dimensions:** Length 94.0-169.2 µm, width 5.7-7.0 µm, fibulae 10 in 10 µm, striae 24-26 in 10 µm.

Nitzschia sigma (Kützing) W.Smith, 1853 (Figures 4.M, 4.N). **References:** Witkowski et al. (2000), pages 854-855, pl. 206, Figures 1-10. **Dimensions:** Length 62.4-69.2 µm, width 5-6.6 µm, fibulae 12 in 10 µm.

Psammodictyon panduriforme (W.Gregory) D.G.Mann, 1990 (Figure 5.B, 5.C). **References:** Witkowski et al. (2000), pages 814-815, pl. 186, Figures 1-3. **Dimensions:** Length 45.5-96.5 µm, width 20.3-31.5 µm, fibulae 8-10 in 10 µm, striae 15-18 in 10 µm, areolae 12-16 in 10 µm.

Psammodictyon sp. (Figure 5.D). **Dimensions:** Length 19.4 µm, width 22 µm, fibulae 11 in 10 µm, areola 32 in 10 µm.

Psammodictyon roridum (M.H.Giffen) D.G.Mann, 1990 (Figure 5.I). **References:** Witkowski et al. (2000), pages 810-811, pl. 184, Figures 9-12. **Dimensions:** Length 41.6 µm, width 13.6 µm, fibulae 14 in 10 µm, striae 24 in 10 µm, areolae 30 in 10 µm. **Comment:** Witkowski et al. (2000) noted as *Bacillaria rorida*.

Tryblionella coarctata Peragallo (Figure 5.E, 5.F). **References:** Witkowski et al. (2000), pages 814-815, pl. 186, Figures 4-13. **Dimensions:** Length 22.4-25.8 µm, width 6.5-8.5 µm, fibulae 11 in 10 µm, striae 22-30 in 10 µm, areola 30 in 10 µm. **Comment:** Basionym *Nitzschia coarctata*.

Tryblionella graeffei (Grunow ex Cleve) D.G.Mann, 1990 (Figure 5.A). **References:** Witkowski et al. (2000), pages 826-827, pl. 192, Figure 1. **Dimensions:** Length 128.8 µm, width 23.7 µm, fibulae 6 in 10 µm, striae 12 in 10 µm, areolae 16 in 10 µm. **Comments:** First record in Bawean Island, basionym *Nitzschia graeffei* Grunow ex Cleve.

Tryblionella sp. (Figure 5.G). **Dimensions:** Length 29.3 µm, width 3.9 µm, fibulae 14 in 10 µm, striae 38 in 10 µm.

Order: Eupodiscales

Pseudictyota dubium (Brightwell) P.A.Sims & D.M.Williams, 2018 (Figures 2.L, 2.M). **References:** López-Fuerte et al. (2020). page 40, Figure 13 (E-K); Beltrones et al. (2021), page 9, Figure 3 (G-I); Beltrones et al. (2023), page 60, Figure A48 (F, G). **Dimensions:** Length 128.8 µm, width 23.7 µm, fibulae 6 in 10 µm, striae 12 in 10 µm, areolae 16 in 10 µm.

Order: Lyrellales

Lyrella cf. *robertsiana* (Greville) D.G.Mann, 1990 (Figure 6.A). **References:** Stidolph et al. (2012), pl. 14, Figures 1, 2. **Dimensions:** Length 93.5 µm, width 43.5 µm, striae 8-12 in 10 µm. **Comment:** This specimen is not to be conspecific with Figure 6 (B-C) in terms of lyra shape and width as well as areolation of the striae. While a1/a2 could be conspecific with '*Navicula robertsiana* f. *typica*' Hustedt 1964 (Hustedt Kieselalgen III, Figure 1544), not only does the varied nomenclature is invalid, but also the species seems to be a bit different from *Navicula robertsiana* Greville 1865 which has been recombined as *Lyrella robertsiana*.

Lyrella hennedyi (W.Smith) Stickle & D.G.Mann, 1990 (Figure 7.I). **References:** Witkowski et al. (2000), pages 632-633, pl. 95, Figure 3. **Dimensions:** Length 31.7 µm, width 20.1 µm, striae 14 in 10 µm, areola 20 in 10 µm. **Comments:** Basionym *Navicula hennedyi* f. *hennedyi* W. Smith.

Lyrella lyra (Ehrenberg) Karajeva, 1978 (Figures 6.B, 6.C). **References:** Foged (1975), pages 110-111, pl. XXIII, Figure 1. **Dimensions:** Length 67.1- 93.5 µm, width 30.7-43.5 µm, striae 8-12 in 10 µm.

Lyrella abrupta (Gregory) D.G.Mann, 1990 (Figures 7.L-7R). **References:** Witkowski et al. (2000), pages 640-641, pl. 99, Figure 8. **Dimensions:** Length 20.0-27.3 µm, width 13.0-17.6 µm, striae 16 in 10 µm. **Comments:** Basionym *Navicula lyra* var. *abrupta* Gregory.

Petroneis cf. *glacialis* (Cleve) Witkowski, Lange-Bertalot & Metzeltin (Figures 7.E, 7.S, 7.T). **References:** Witkowski et al. (2000), pages 644-645, pl. 101, Figure 1; pages 646-647, pl. 102, Figure 4. **Dimensions:** Length 25.3-29.9 µm, width 17.2-19.2 µm, striae 18 in 10 µm, areola 15 in 10 µm. **Comments:** This specimen has extended apical raphe endings, which are bent in the same direction. This is also comparable to *Petroneis glacialis* yet with smaller size and denser striae.

Petroneis marina Round et al. 1990 (Figures 7.A, 7.B). **References:** Witkowski et al. (2000), pages 646-647, pl. 102, Figure 1. **Dimensions:** Length 35.7-65.4 µm, width 19.9-25.4 µm, striae 12 in 10 µm, areolae 10 in 10 µm.

Petroneis granulata (Bailey) D.G.Mann, 1990 (Figure 7.C). **References:** Park et al. (2018), page 108, Figure 27; Al-Handal et al. (2018), page 118, Figure 18. **Dimensions:** Length 44.1 µm, width 21.7 µm, striae 12 in 10 µm, areolae 10 in 10 µm. **Comment:** Basionym *Navicula granulata* Bailey. Algaebase.org noted as *Petroneis granulata* D.G.Mann, nom. illeg. (illegitimate names).

Order: Mastogloiales

Mastogloia binotata (Grunow) Cleve, 1895 (Figure 3.R). **References:** Witkowski et al. (2000), pages 592-593, pl. 75, Figures 15-17. **Dimensions:** Length 24.1 µm, width 17.3 µm, striae 16 in 10 µm, areolae 12 in 10 µm.

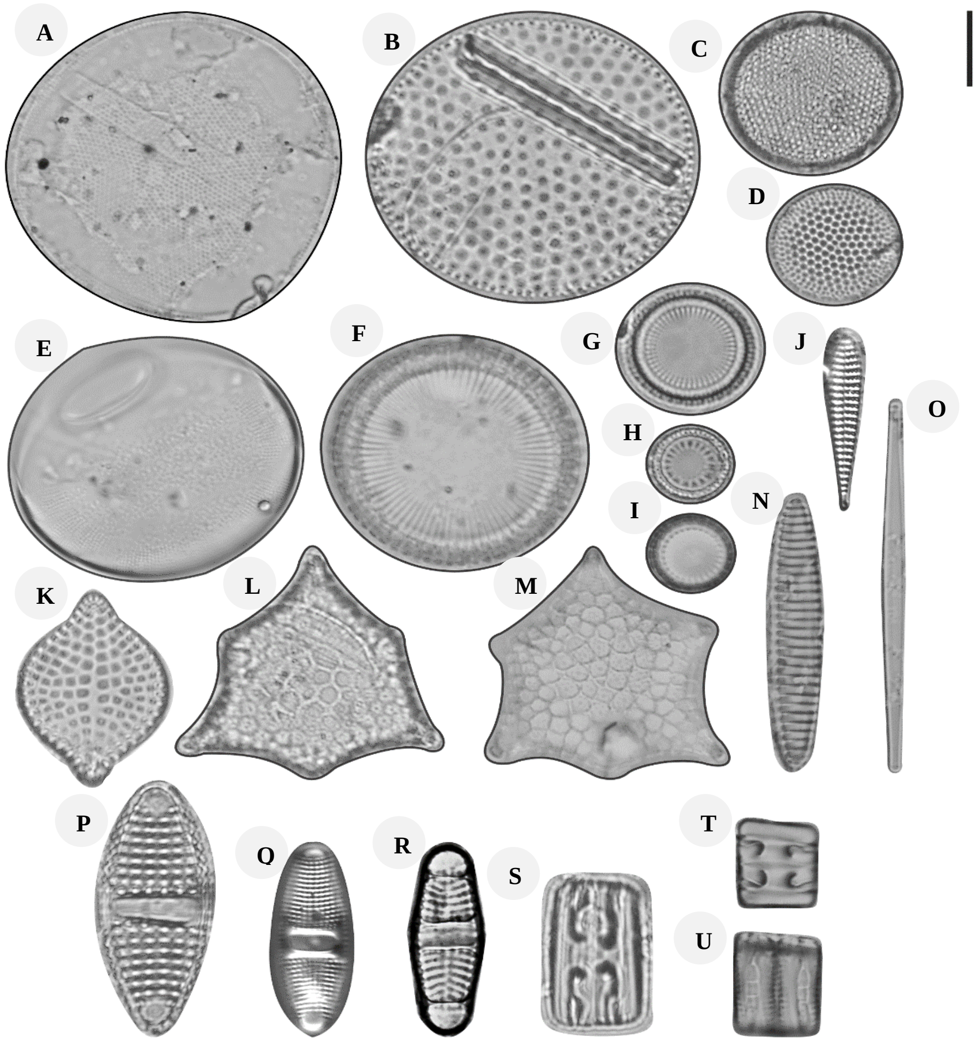

Figure 1. A. *Hyalodiscus scoticus*; B. *Psammodiscus nitidus*; C, D. *Thalassiosira* sp.; E. *Actinocyclus subtilis*; F-I. *Paralia sulcata*; J. *Trachysphenia* sp.; K. *Rhaphoneis* cf. *amphiceros*; L-M. *Pseudictyota dubium*; N. *Fragilariopsis* sp.; O. *Tabularia fasciculata*; P. *Plagiogramma staurophorum*; Q. *Plagiogramma pulchellum*; R. *Plagiogramma rhombicum*; S. *Grammatophora marina* var. *undata*; T. *Grammatophora angulosa* var. *islandica*; U. *Mastogloia* sp. Scale bar: 10 µm. LM: x1500

Mastogloia crucicula (Grunow) Cleve, 1895 (Figure 3.Q). **References:** Witkowski et al. (2000), 592-593, pl. 75, Figure 3. **Dimensions:** Length 15 µm, width 7.8 µm, striae 20 in 10 µm.

Mastogloia macdonaldii Greville, 1865 (Figure 3.S). **References:** Witkowski et al. (2000), pages 598-599, pl. 78, Figures 7, 8. **Dimensions:** Length 30.7 µm, width 13.2 µm, striae 24 in 10 µm.

Mastogloia manokwariensis Cholnoky, 1963 (Figure 3.P). **References:** Witkowski et al. (2000), pages 602-603, pl. 80, Figure 11. **Dimensions:** Length 14.6 µm, width 6.3 µm, striae 28 in 10 µm.

Mastogloia sp. (Figure 2.U). **Dimensions:** Length 13.3 µm, width 9.6 µm, striae 14 in 10 µm. **Comment:** Visible partecta in girdle view side.

Order: Naviculales

Biremis ambigua (Cleve) D.G.Mann, 1990 (Figures 13.E, 13.I). **References:** Witkowski et al. (2000), pages 752-753, pl. 155, Figures 2-6. **Dimensions:** Length 39.1-45.3 µm, width 6.4-10.5 µm.

Climaconeis lorenzii Grunow, 1862 (Figures 13.C, 13.D). **References:** López-Fuerte et al. (2022), page 23, Figure 10 (N, O). **Dimensions:** Length 82.9-105.9 µm, width 6.1-66.0 µm, striae 2 in 10 µm, areolae 20-22 in 10 µm.

Diademoides luxuriosa (Greville) K.-D.Kemp & T.B.B.Paddock, 1990 (Figure 7.D). **References:** Kemp and Paddock (1990), page 1. **Dimensions:** Length 35.7 µm, width 19.9 µm, striae 12 in 10 µm, areolae 10 in 10 µm. **Comments:** This specimen has featured an undivided parietal chamber, with large areolae embedded in the chamber walls. The species is the only member of the genus with original report from Australia.

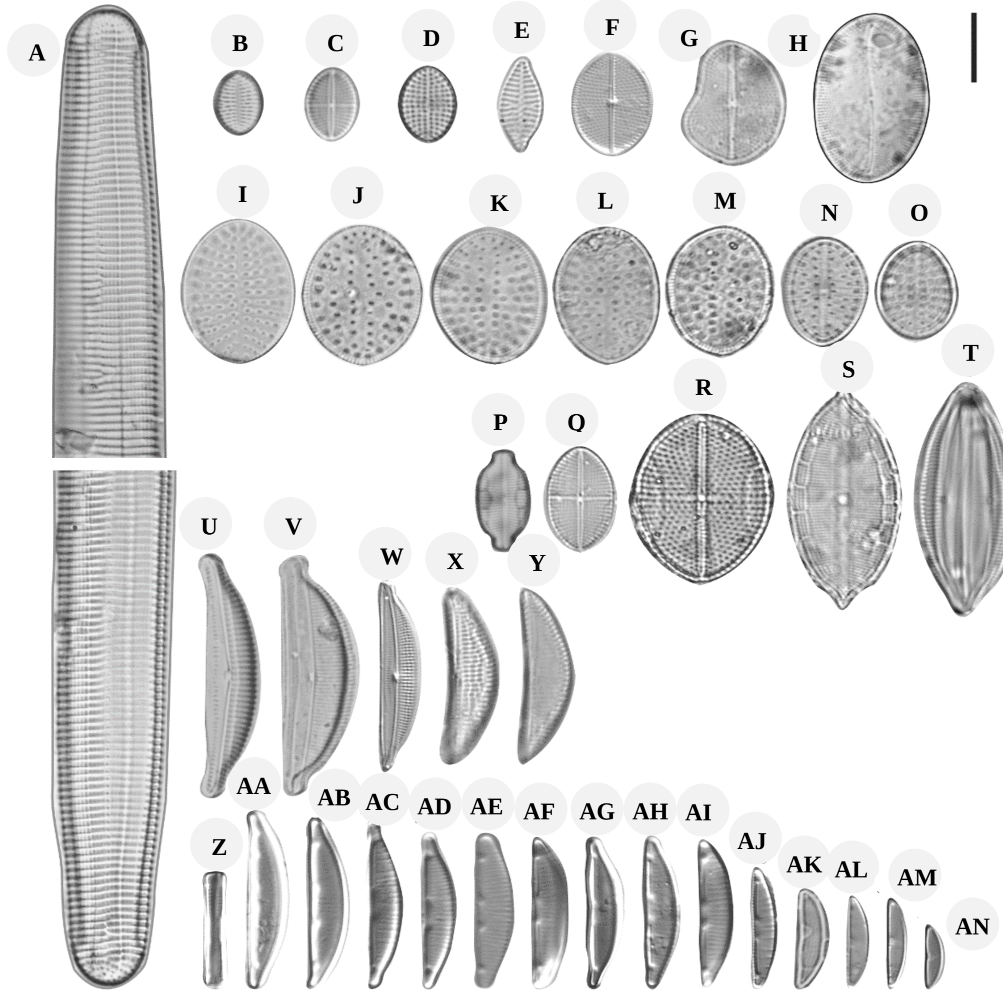

Figure 2. A. *Ardissonea robusta*; B. *Amphicocconeis disculoides*; C. *Cocconeis stauroneiformis*; D. *Cocconeis scutellum*; E. *Planothidium campechianum*; F. *Cocconeis* sp.; G. *Cocconeiopsis* (cf.) *regularis*; H. *Cocconeis krammeri*; I-O. *Cocconeis guttata*; P. *Mastogloia manokwariensis*; Q. *Mastogloia crucicula*; R. *Mastogloia binotata*; S. *Mastogloia macdonaldii*; T. *Amphora* sp. (*sensu lato*); U. *Amphora* sp. 11; V. *Amphora* sp. 12; W. *Amphora* sp. 13; X, Y. *Amphora* sp. 14; Z. *Catenula* sp. (*Catenula decusa*); AA-AC. *Catenula* sp. 1 (*Paracatenula porostriata*); AD, AE, AH, AI. *Catenula javanica*; AF, AG. *Catenula adhaerens*; AJ. *Catenula* sp. 2 (*Catenula boyanensis*); AK. *Catenulopsis catenulafalsa*; AL-AN. *Catenula* sp. 3 (*Catenula densestriata*). Scale bar: 10 µm. LM: x1500

Diploneis cf. *biremiformis* S.J.M.Droop, 1998 (Figure 7.F). **References:** Droop (1998), page 345, Figure 27; page 353, Figures 48-50. **Dimensions:** Length 14.9 µm, width 6.9 µm, striae 16 in 10 µm.

Diploneis cf. *mediterranea* (Grunow) Cleve, 1894 (Figures 9.A-9.E). **References:** Cleve (1894), page 82. **Dimensions:** Length 39.0-72.5 µm, width 14.5-17.5 µm, striae 7-10 in 10 µm.

Diploneis cf. *pneumatica* S.J.M.Droop, 1998 (Figure 7.G). **References:** Witkowski et al. (2000), pages 616-617, pl. 87, Figure 12. **Dimensions:** Length 11.9 µm, width 6.2 µm, striae 20 in 10 µm.

Diploneis chersonensis Grove (Figure 8.C). **References:** Lobban et al. (2012), page 428, pl. 44, Figures 1-4. **Dimensions:** Length 61.2 µm, width 18.9 µm, striae 11 in 10 µm, areola 2 in 10 µm.

Diploneis coffeiformis (A.W.F.Schmidt) Cleve (Figure 9.G). **References:** López-Fuerte et al. (2024), page 14, Figure 8 (I). **Dimensions:** Length 18.7 µm, width 11.9 µm, striae 12 in 10 µm.

Diploneis crabro (Ehrenberg) Ehrenberg, 1854 (Figures 8.A, 8.B). **References:** Lobban et al. (2012), page 428, pl. 44, Figure 5. **Dimensions:** Length 45.3-73.7 µm, width 14.7-24.2 µm, striae 7-13 in 10 µm.

Diploneis littoralis (Donkin) Cleve, 1894 (Figures 9.N-9.P). **References:** Witkowski et al. (2000), pages 620-621, pl. 89, Figure 3. **Dimensions:** Length 36.2-41.1 µm, width 20.0-21.7 µm, striae 12 in 10 µm, areola 10 in 10 µm.

Diploneis (cf.) *litoralis* var. *clathrata* (Ostr.) Cleve, 1896 (Figure 8.F). **References:** Witkowski et al. (2000), pages 620-621, pl. 89, Figures 5, 7-13. **Dimensions:** Length 32 µm, width 11 µm, striae 12 in 10 µm, areola 10 in 10 µm.

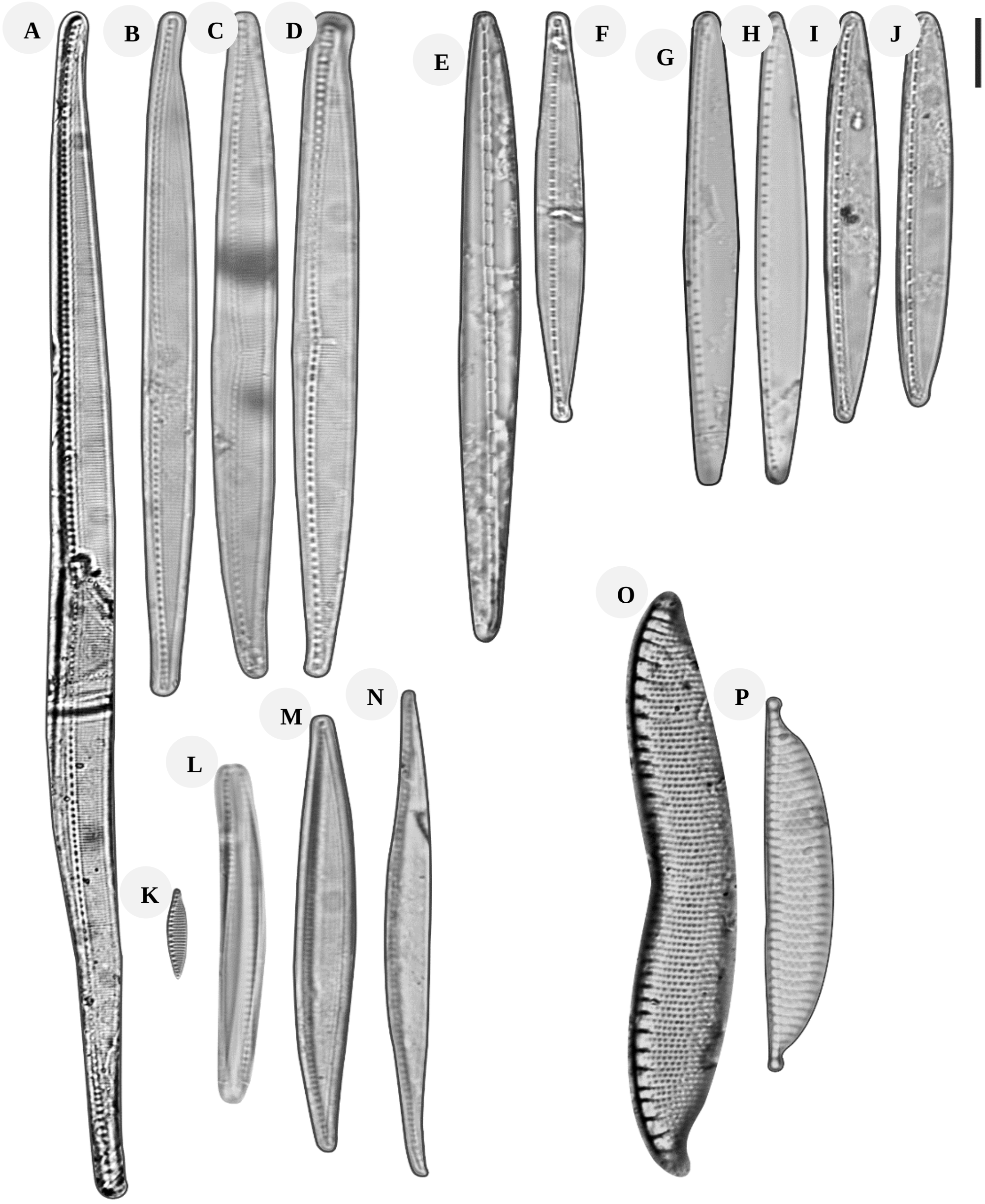

Figure 3. A-D. *Nitzschia scalpelliformis*; E. *Bacillaria socialis*; F. *Bacillaria paxillifer*; G-I. *Nitzschia filiformis*; K. *Nitzschia liebethruthii*; L. *Nitzschia distans*; M, N. *Nitzschia sigma*; O. *Hantzschia virgata*; P. *Hantzschia kaiseri*. Scale bar: 10 µm. LM: x1500

Diploneis notabilis (Greville) Cleve, 1894 (Figure 9.M). **References:** Witkowski et al. (2000), pages 620-621, pl. 89, Figures 15-21; Kryk (2016), page 98, pl. 10, Figure 294. **Dimensions:** Length 45.3 µm, width 30 µm, striae 11 in 10 µm.

Diploneis smithii (Brébisson) Cleve, 1894 (Figures 8.G-8.J). **References:** Lobban et al. (2012), page 430, pl. 45, Figures 3-6. **Dimensions:** Length 37.2-64.1 µm, width 17.6-25 µm, striae 9 in 10 µm.

Diploneis sp. 1 (Figure 9.F). **Dimensions:** Length 40.1 µm, width 10.3 µm, striae 8 in 10 µm.

Diploneis sp. 2 (Figures 9.H, 9.I). **Dimensions:** Length 33.6-47.5 µm, width 11.8-14.7 µm, striae 8-10 in 10 µm.

Diploneis sp. 3 (Figure 9.J). **Dimensions:** Length 45.3 µm, width 19.5 µm, striae 13 in 10 µm.

Diploneis sp. 4 (Figures 9.K, 9.L). **Dimensions:** Length 51.4 µm, width 15 µm, striae 10 in 10 µm, areolae 20 in 10 µm. **Comments:** Figure 9 (k and l) same specimen with different focal planes.

Diploneis vacillans (A.Schmidt) Cleve, 1894 (Figures 8.D, 8.E). **References:** Kryk (2016), page 98, pl. 10, Figures 291-293. **Dimensions:** Length 32.0-50.7 µm, width 11.0-14.7 µm, striae 10-12 in 10 µm.

Fallacia cf. *nummularia* (Greville) D.G.Mann, 1990 (Figure 7.J). **References:** Witkowski et al. (2000), pages 584-585, pl. 71, Figures 10, 11. **Dimensions:** Length 29.6 µm, width 21 µm, striae 14 in 10 µm.

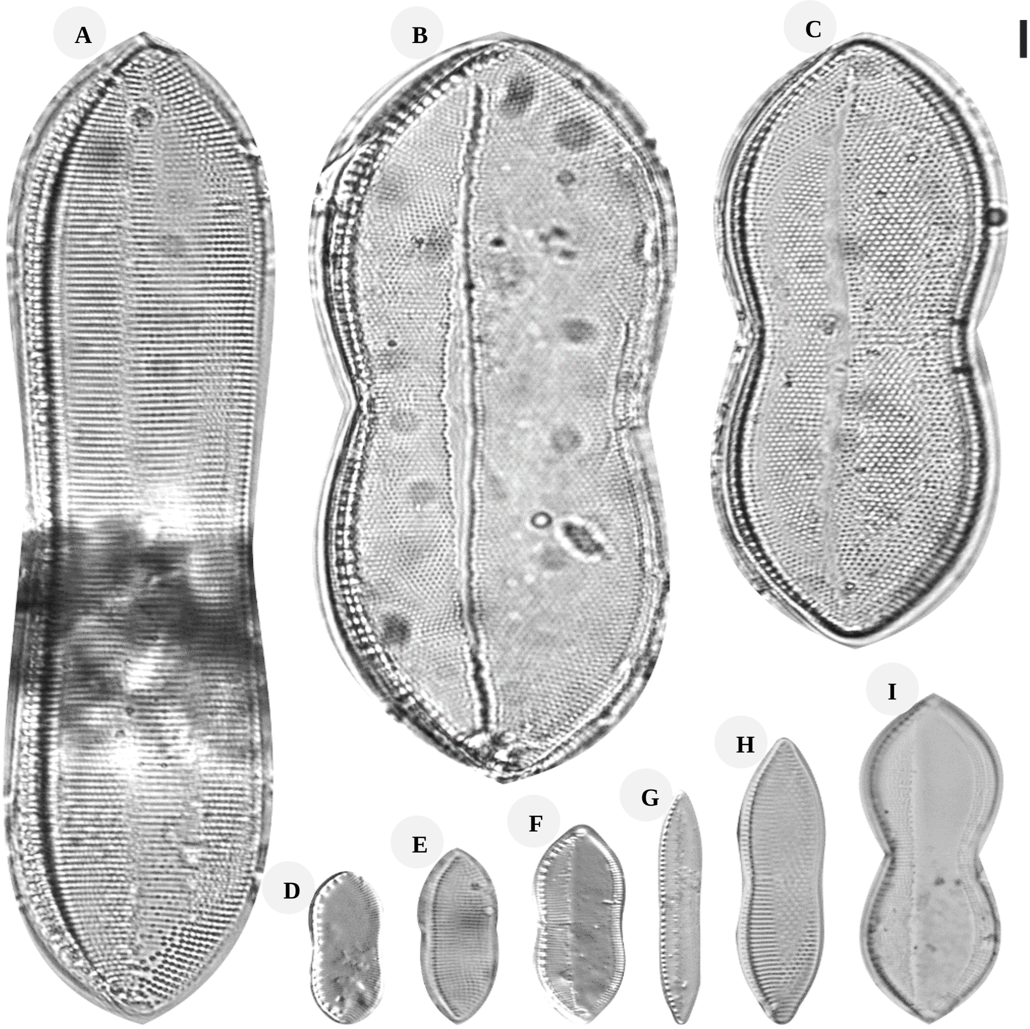

Figure 4. A. *Tryblionella graeffei*; B-C. *Psammodictyon panduriforme*; D. *Psammodictyon* sp; E-F. *Tryblionella coarctata*; G. *Tryblionella* sp.; H. *Nitzschia* cf. *coarctata*; I. *Psammodictyon roridum*. Scale bar: 10 µm. LM: x1500

Fallacia nyella (Hustedt) D.G.Mann, 1990 (Figure 7.N). **References:** Witkowski et al. (2000), pages 582-583, pl. 70, Figures 1-7. **Dimensions:** Length 12.7 µm, width 7.2 µm, striae 28 in 10 µm. **Comment:** Basionym *Navicula nyella*.

Gyrosigma cf. *plagiostomum* (Grunow) Cleve (Figure 13.B). **References:** Meister (1932), page 29, Figure 66. **Dimensions:** Length 88.5 µm, width 13 µm, transapical striae 16 in 10 µm, longitudinal striae 18 in 10 µm, raphe angle +7. **Comments:** Also recorded in Sabang Island, Aceh, Indonesia.

Halamphora coffeiformis (C.Agardh) Mereschk. (Figures 10.A-10.E; 11.N). **References:** Witkowski et al. (2000), pages 776-777, pl. 167, Figure 3. **Dimensions:** Length 24.5-39.3 µm, width 5.5-9.1 µm, dorsal striae 16-20 in 10 µm, ventral striae 25-35 in 10 µm.

Halamphora holsatica (Hustedt) Levkov, 2009 (Figures 10.F-10.I, 10.R-10.T). **References:** Levkov (2009), pages 522-523, pl. 101, Figures 1-11; pages 782-783, pl. 227, Figures 1-6; Al-Handal et al. (2016), page 64, pl. 8, Figures 2, 3. **Dimensions:** Length 23.7-32.6 µm, width 6.4-8.2 µm, striae 13-14 in 10 µm. **Comment:** Al-Handal et al. (2016) noted as *Amphora holsatica*.

Halamphora interupta (Heiden) Levkov, 2009 (Figures 10.L, 10.M, 10.AC). **References:** Levkov (2009), pages 550-551, pl. 113, Figures 13-15. **Dimensions:** Length 27.8-52.1 µm, width 8.4-10.9 µm, striae 12 in 10 µm.

Halamphora kolbei (Aleem) Ãlvarez-Blanco & S.Blanco, 2014 (Figure 10.Z). **References:** Witkowski et al. (2000), pages 768-769, pl. 163, Figure 26. **Dimensions:** Length 11.8 µm, width 3.4 µm.

Haslea nautica (Cholnoky) Giffen, 1980 (Figure 11.J). **References:** Al-Handal et al. (2016), page 66, pl. 9, Figure 4. **Dimensions:** Length 48.3 µm, width 9.3 µm.

Hippodonta sp. (Figure 11.M). **Dimensions:** Length 14.6 µm, width 4.9 µm, striae 5 in 10 µm.

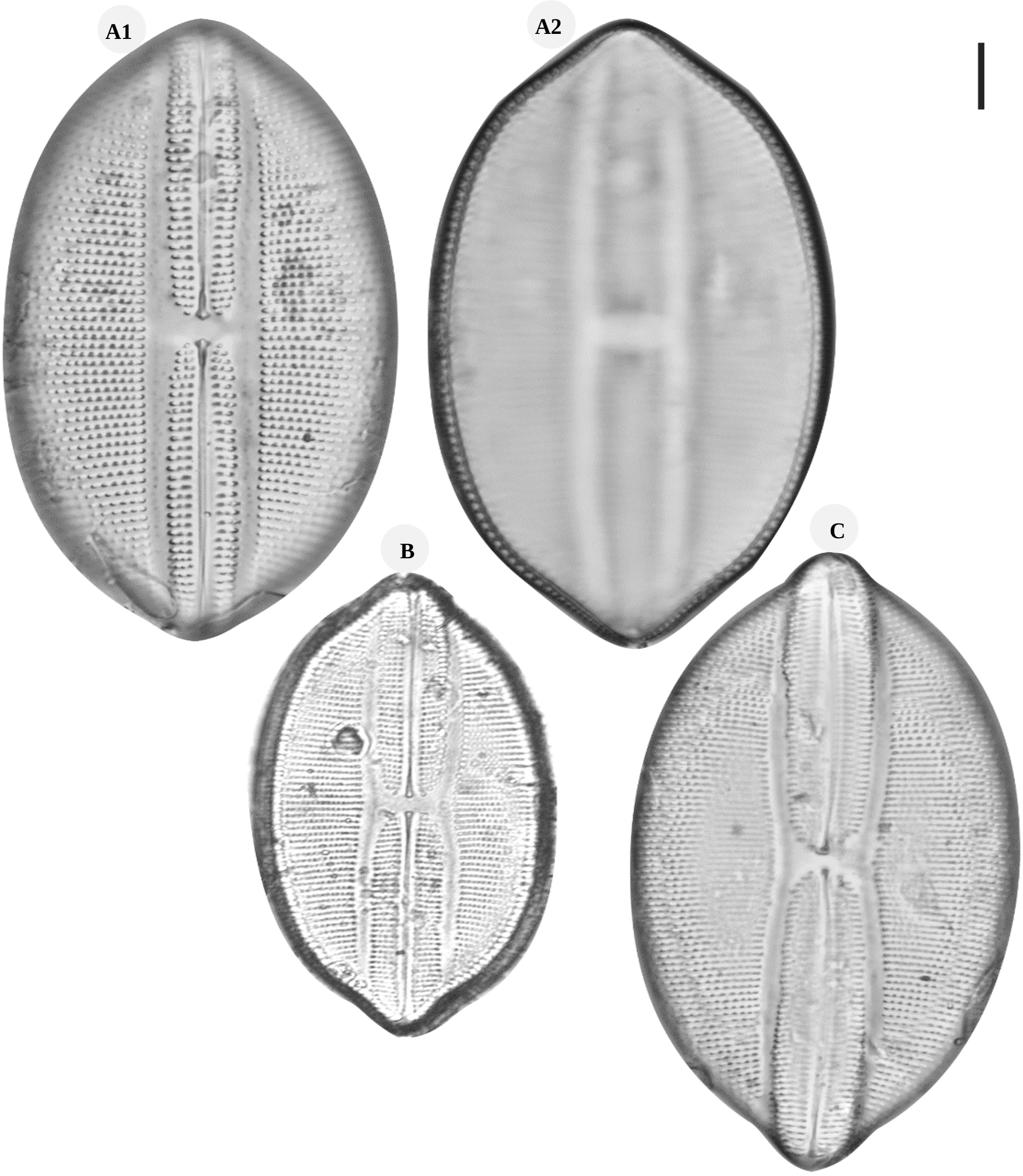

Figure 5. A1 = A2. *Lyrella* cf. *robertisiana*; B, C. *Lyrella lyra.* Scale bar: 10 µm. LM: x1500

Hippodonta sp. (Figure 11.L). **Dimensions:** Length 20.2 µm, width 4.9 µm, dorsal striae 12 in 10 µm, ventral striae 20 in 10 µm. **Comments:** Girdle view.

Lunella sp. (Figure 11.S). **References:** Kryk (2016), page 95, pl. 7, Figures 182, 183. **Dimensions:** Length 26.9 µm, width 6.5 µm, striae 18 in 10 µm. **Comments:** This specimen is similar to Gen. et. sp. nov. indet. 4 Kryk (2016).

Lyrella sp. (Figure 7.K). **Dimensions:** Length 35.1 µm, width 17 µm, striae 14 in 10 µm.

Navicula (cf.) *viminoides* M.F.Giffen (Figure 11.T). **References:** Giffen (1975), pl. III, Figures 99-101. **Dimensions:** Length 15.7 µm, width 7.3 µm, striae 14 in 10 µm, areolae 25 in 10 µm.

Navicula athenea Witkowski, Lange-Bertalot, Metzeltin (Figure 11.V). **References:** Witkowski et al. (2000), pages 700-701, pl. 129, Figures 15, 16. **Dimensions:** Length 18.6 µm, width 6.9 µm, striae 10 in 10 µm.

Navicula carinifera Grunow (Figure 11.K). **References:** Al-Handal et al. (2018), page 125, Figures 46-48. **Dimensions:** Length 39.9 µm, width 12.7 µm, striae 14 in 10 µm.

Navicula directa (W.Smith) Brébisson (Figures 11.A, 11.B). **References:** Witkowski et al. (2000), pages 700-

701, pl. 129, Figure 1. **Dimensions:** Length 52.4-70.8 µm, width 9.2-10.0 µm, striae 8-10 in 10 µm, areolae 25-30 in 10 µm.

Navicula kariana var. *frigida* (Grunow) Cleve (Figure 11.I). **References:** Witkowski et al. (2000), pages 706-707, pl. 132, Figures 11-14. **Dimensions:** Length 52.8 µm, width 16.2 µm, striae 22 in 10 µm.

Navicula mollis (W.Smith) Cleve (Figures 11.F-11.H). **References:** Witkowski et al. (2000), pages 726-727, pl. 142, Figure 36. **Dimensions:** Length 40.6-55.3 µm, width 9-9.4 µm, striae 8 in 10 µm, areolae 30 in 10 µm.

Navicula sp. 1 (Figure 11.C). **Dimensions:** Length 63.2 µm, width 8.5 µm, striae 10 in 10 µm, areolae 25 in 10 µm.

Navicula sp. 2 (Figures 11.D, 11.E). **Dimensions:** Length 47.5-59.7 µm, width 8.0-8.4 µm, striae 10-11 in 10 µm, areolae 25 in 10 µm.

Navicula sp. 3 (Figure 11.U). **Dimensions:** Length 18.6 µm, width 7.6 µm, striae 12 in 10 µm.

Parlibellus delognei (Van Heurck) E.J.Cox, 1988 (Figures 11.P-11.R). **References:** Witkowski et al. (2000), pages 650-651, pl. 104, Figures 1-5. **Dimensions:** Length 27.6-33.4 µm, width 9.3-10.4 µm, striae 22 in 10 µm, areolae 25 in 10 µm.

Parlibellus sp. (Figure 13.F). **Dimensions:** Length 28.8 µm, width 8.8 µm, striae 9 in 10 µm, areolae 16 in 10 µm. **Comment:** Valves are linear, elliptic, broadly apices, raphe straight, terminal raphe ends distant from each other, central area wide depressed with 2-3 striae. Transapical striae are punctate and parallel. In some point similar to *Dickieia*, and *Pinnularia*, but *Dickieia* has rectangular fascia, transapical slightly radiate. *Pinnularia* also has wide transversely expanded fascia in the central area.

Parlibellus sp. (Figure 13.M). **Dimensions:** Length 28.8 µm, width 9.4 µm. **Comments:** The valve has broadly rounded apices, raphe straight, and raphe ends bent to the same side. Striation is not visible.

Plagiotropis sp. 1 (Figure 13.K). **Dimensions:** Length 43.4 µm, width 8.4 µm.

Plagiotropis sp. 2 (Figure 13.L). **Dimensions:** Length 37.4 µm, width 9.8 µm.

Pleurosigma sp. (Figure 13.A). **References:** Plinski and Witkowski (2020), pages 306-307, Figure 459. **Dimensions:** Length 158.4 µm, width 22.3 µm, transverse striae 18 in 10 µm, diagonal striae 22 in 10 µm, raphe angle +9.7. **Comments:** The specimen closely resembles *Pleurosigma angulatum*, with a valve width of 30-60 µm.

Sellaphora sp. (Figure 12.F). **Dimensions:** Length 45.3 µm, width 10.5 µm. **Comments:** The specimen is similar to *Pinnunavis genustriata*, but the striae of the genus *Pinnunavis* are not areolate.

Seminavis robusta D.B.Danielidis & D.G.Mann, 2002 (Figure 11.O). **References:** Danielidis and Mann (2002), page 440, Figures 39-47. **Dimensions:** Length 24.7-47.9 µm, width 4.9-10.2 µm, dorsal striae 16-30 in 10 µm, ventral striae 16-22 in 10 µm. **Comments:** The specimen is similar to *Seminavis ventricosa*, which has slender specimens with very narrow ventral striae. Very similar specimens have also been found on Java Island (Danielidis and Mann 2002).

Seminavis strigosa (Hustedt) Danieledis & Economou-Amilli, 2003 (Figure 13.H). **References:** Danielidis and Mann (2003), page 30, Figures 23-26. **Dimensions:** Length 38.2 µm, width 4.8 µm, dorsal striae 16 in 10 µm, ventral striae 12 in 10 µm.

Trachyneis aspera (Ehrenberg) Cleve, 1894 (Figures 12.A-12.D). **References:** Beltrones et al. (2021), page 27, Figure 21 (I). **Dimensions:** Length 40.0-138.5 µm, width 10.5-31.4 µm.

Trachyneis aspera ((Ehrenberg) Cleve, 1894 (Figure 12.E). **References:** Witkowski et al. (2000), pages 760-761, pl. 159, Figures 1-6. **Dimensions:** Length 53.8 µm, width 16.9 µm, striae 14 in 10 µm. **Comments:** Girdle view.

Trachyneis velata A.Schmidt (Figures 12.G-12.I). **References:** Witkowski et al. (2000), pages 760-761, pl. 159, Figures 7, 8. **Dimensions:** Length 56.0-76.9 µm, width 12.1-19.5 µm.

Order: Rhopalodiales

Epithemia gibberula var. *baltica* (O.Müller) J.S.Park & Lobban (Figures 14.H, 14.I). **References:** Park et al. (2022), page 47, Figures 61-62. **Dimensions:** Length 37.8-47.6 µm, width 10 µm, striae 10 in 10 µm.

Epithemia gracilis Gerd Moser, 1998 (Figure 14.J). **References:** Moser (1998), page 158, pl. 65, Figures 1-9. **Dimensions:** Length 28.9 µm, width 8.9 µm, striae 4 in 10 µm.

Epithemia guettingeri (Krammer) Lobban & Park (Figures 14.K, 14.L). **References:** Park et al. (2018), page 133, Figures 171-173. **Dimensions:** Length 18.9-23.0 µm, width 5.9-6.4 µm, striae 9 in 10 µm.

Order: Surirellales

Auricula intermedia (Lewis) Cleve, 1894 (Figure 13.J). **References:** Al-Handal et al. (2018), page 140, Figure 102. **Dimensions:** Length 48.7 µm, width 12.4 µm.

Campylodiscus neofastuosus Ruck & Nakov (Figures 14.A-14.D). **References:** Beltrones et al. (2021), page 40, Figure 34 (A-D). **Dimensions:** Length 30.6-38.0 µm, width 25.8-30.3 µm, fibulae 4 in 10 µm.

Coronia decora (Brébisson) Ruck & Guiry (Figures 14.E-14.G). **References:** Witkowski et al. (2000), pages 870-871, pl. 214, Figure 15; Lobban et al. (2012), page 306, pl. 65, Figures 1, 2. **Dimensions:** Length 6.4-49.0 µm, width 4.8-38.2 µm, striae 4-16 in 10 µm. **Comment:** Witkowski et al. (2000) noted as *Campylodiscus decorus*.

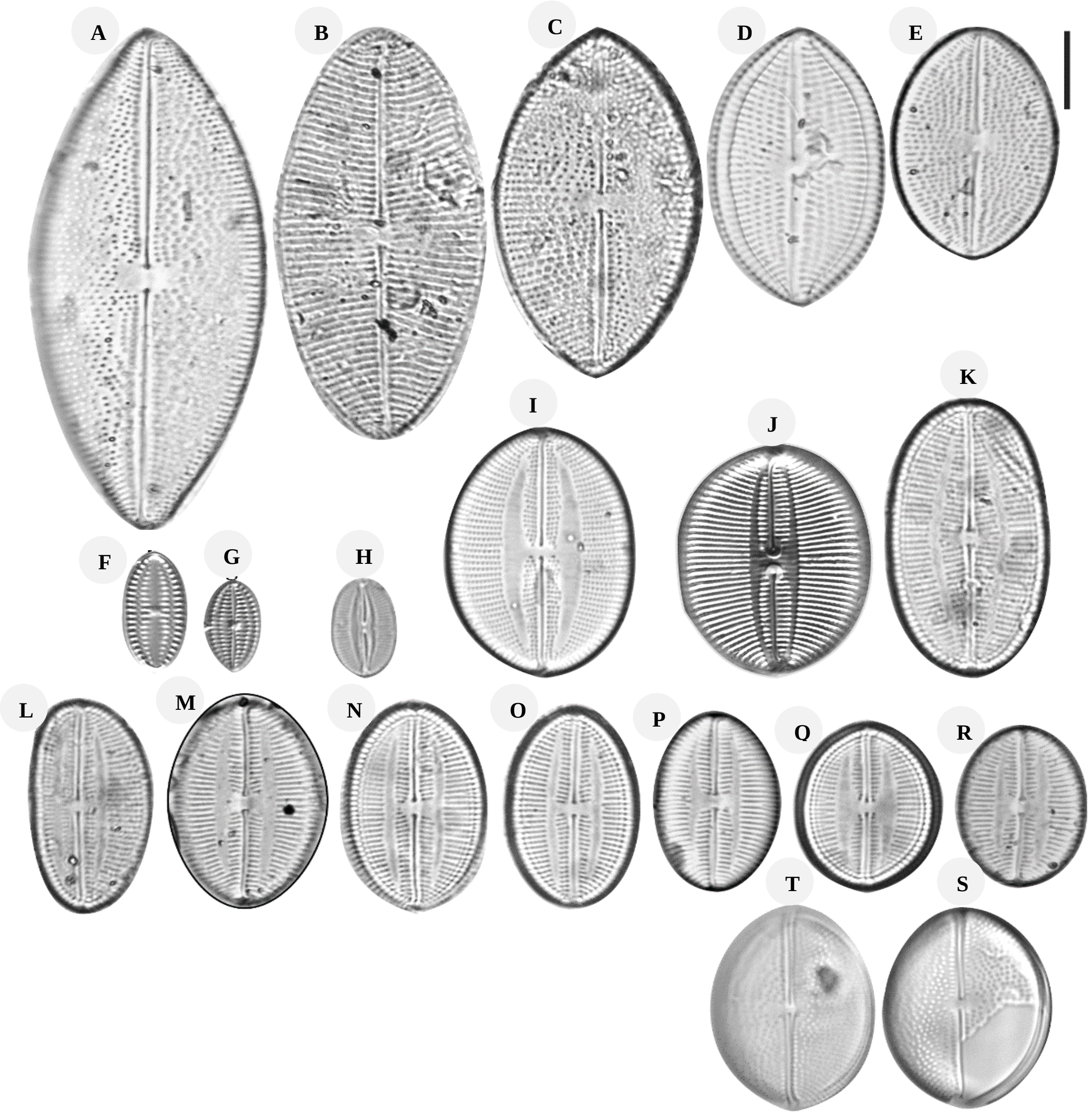

Figure 6. A, B. *Petroneis marina*; C. *Petroneis granulata*; D. *Diademoides luxuriosa*; E, S, T. *Petroneis* cf. *glacialis*; F. *Diploneis* cf. *biremiformis*; G. *Diploneis* cf. *pneumatica*; H. *Fallacia nyella*; I. *Lyrella hennedyi*; J. *Fallacia nummularia*; K. *Lyrella* sp.; L-R. *Lyrella abrupta*. Scale bar: 10 µm. LM: x1500

Petrodictyon gemma (Ehrenberg) D.G.Mann, 1990 (Figure 14.M). **References:** Witkowski et al. (2000), pages 874-875, pl. 216, Figures 8, 9. **Dimensions:** Length 30.6-38.0 µm, width 25.8-30.3 µm, fibulae 4 in 10 µm.

Plagiodiscus nervatus Grunow, 1978 (Figure 14.N). **References:** Park et al. (2018), page 133, Figures 168, 169. **Dimensions:** Length 31.2 µm, width 21 µm, fibulae 4 in 10 µm.

Order: Thalassiophysales

Amphora amoena Hustedt, 1955 (Figures 10.P, 10.Q). **References:** Witkowski et al. (2000), pages 776-777, pl. 167, Figure 11. **Dimensions:** Length 20.1 µm, width 5.4 µm, dorsal striae 18 in 10 µm.

Amphora egregia var. *interupta* H. Peragallo & M. Peragallo (Figure 10.AB). **References:** Peragallo and Peragallo (1897), pl. XLVI, Figures 6, 7, 11. **Dimensions:** Length 64.5 µm, width 7.9 µm, dorsal striae 10 in 10 µm.

Amphora marina Ralfs, 1861 (Figure 10.AE). **References:** Beltrones et al. (2021), page 32, Figure 26 (H, I). **Dimensions:** Length 48.4 µm, width 11 µm, dorsal striae 10 in 10 µm, ventral striae 12 in 10 µm.

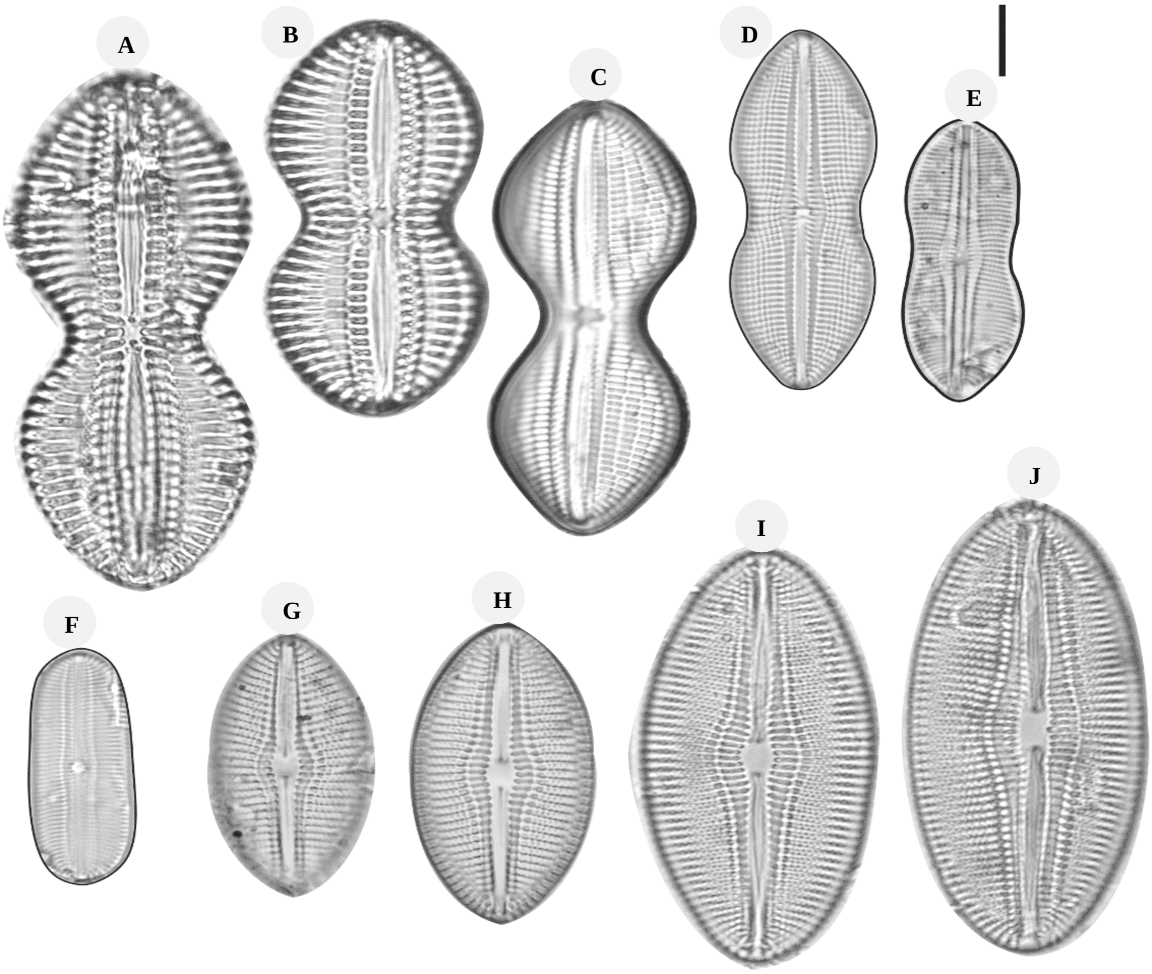

Figure 7. A, B. *Diploneis crabro*; C. *Diploneis chersonensis*; D, E. *Diploneis vacillans*; F. *Diploneis* (cf.) *litoralis* var. *clathrata*; G-J. *Diploneis smithii*. Scale bar: 10 µm. LM: x1500

Amphora montgomeryi A.H.Wachnicka & E.E.Gaiser, 2007 (Figures 10.O, 10.W). **References:** Wachnicka and Gaiser (2007), page 413, Figures 84-86. **Dimensions:** Length 19.3-20.1 µm, width 5.5-6.7 µm, dorsal striae 18 in 10 µm.

Amphora ostrearia Brébisson, 1849 (Figure 10.AF). **References:** Witkowski et al. (2000), pages 782-783, pl. 170, Figure 23. **Dimensions:** Length 44.2 µm, width 11 µm, dorsal striae 20 in 10 µm, ventral striae 14 in 10 µm.

Amphora sp. 2 (Figure 10.J). **Dimensions:** Length 22.3 µm, width 5.2 µm, dorsal striae 22 in 10 µm.

Amphora sp. 3 (Figure 10.U). **Dimensions:** Length 20 µm, width 4.6 µm, dorsal striae 14 in 10 µm, ventral striae 14 in 10 µm.

Amphora sp. 4 (Figure 10.V). **Dimensions:** Length 20.2 µm, width 4.8 µm, dorsal striae 18 in 10 µm, ventral striae 26 in 10 µm.

Amphora sp. 5 (Figure 10.AA). **Dimensions:** Length 62.8 µm, width 10.1 µm, dorsal striae 11 in 10 µm, ventral striae 11 in 10 µm. **Comment:** This taxon resembles *Amphora spectabilis* with raphe slits closer to the dorsal side - see Witkowski et al. (2000) pages 774-775, pl. 166, Figure 8, while in the other plate (pages 776-777, pl. 167, Figures 25-26), the raphe is closer to the ventral side.

Amphora sp. 6 (Figure 10.X). **Dimensions:** Length 26.3 µm, width 5.8 µm, dorsal striae 17 in 10 µm.

Amphora sp. 7 (Figure 10.Y). **Dimensions:** Length 22.9 µm, width 5.6 µm, dorsal striae 10 in 10 µm.

Amphora sp. 9 (Figure 10.AD). **Dimensions:** Length 50.4 µm, width 11.3 µm, dorsal striae 12 in 10 µm.

Amphora sp. 10 (Figures 10.AG-10.AH). **Dimensions:** Length 30.7-36.1 µm, width 10.8-12 µm, dorsal striae 12 in 10 µm, ventral striae 12 in 10 µm.

Amphora sp. 11 (Figure 3.U). **Dimensions:** Length 34.4 µm, width 5.9 µm, dorsal striae 14 in 10 µm, ventral striae 18 in 10 µm.

Amphora sp. 12 (Figure 3.V). **Dimensions:** Length 33.9 µm, width 8.3 µm, dorsal striae 20 in 10 µm.

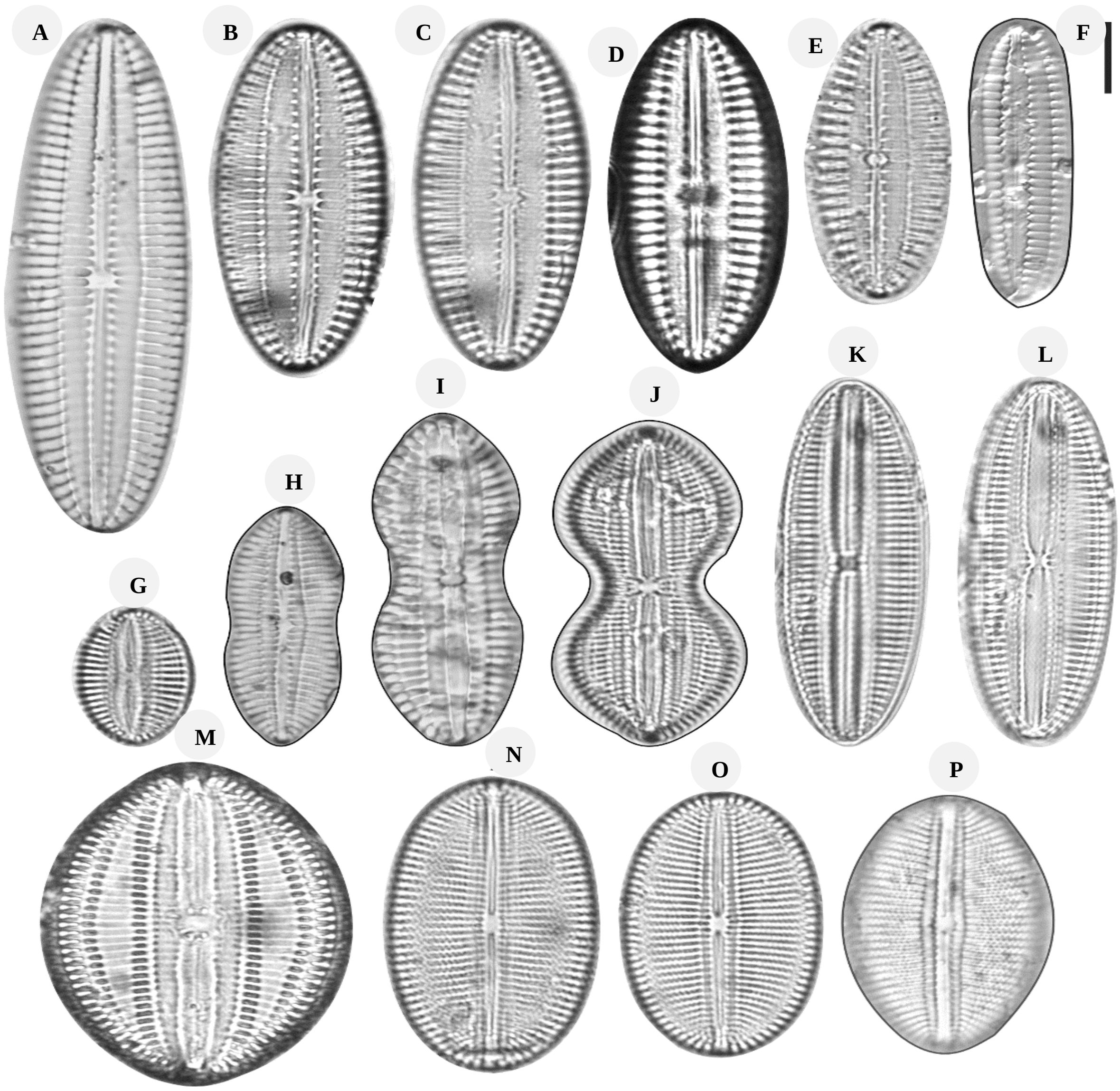

Figure 8. A-E. *Diploneis cf. mediterranea*; F. *Diploneis* sp. 1; G. *Diploneis coffaeiformis*; H, I. *Diploneis* sp. 2; J. *Diploneis* sp. 3; K, L. *Diploneis* sp. 4; M. *Diploneis notabilis*; N-P. *Diploneis littoralis*. Scale bar: 10 µm. LM: x1500

Amphora sp. 13 (Figure 3.W). **Dimensions:** Length 27 µm, width 4.8 µm, dorsal striae 24 in 10 µm, ventral striae 32 in 10 µm.

Amphora sp. 14 (Figure 14.X, 14.Y). **Dimensions:** Length 24.3-25.2 µm, width 5.6-6 µm, dorsal striae 16-20 in 10 µm, ventral striae 16 in 10 µm.

Amphora sp. (*sensu lato*) (Figure 3.T). **Dimensions:** Length 35.7-65.4 µm, width 19.9-25.4 µm, striae 12 in 10 µm, areolae 10 in 10 µm.

Amphora sp. nov. (Figure 10.K). **Dimensions:** Length 22 µm, width 5.2 µm. **Comments:** Frustule with 4 sinusoidal gibbosities on dorsal valve margins.

Catenula adhaerens (Mereschkowsky) Mereschkowsky, 1903 (Figures 3.AF, 3.AG). **References:** Kryk et al. (2021), page 10, Figures 69-104. **Dimensions:** Length 21.1-21.6 µm, width 4.2-4.4 µm.

Catenula javanica Witkowski, Kryk, Risjani & Yunianta (Figures 3.AD, 3.AE, 3.AH, 3.AI). **References:** Kryk et al. (2021), page 8, Figures 49-68. **Dimensions:** Length 20-22 µm, width 4.0-4.6 µm.

Catenula sp. (Figure 3.Z). Dimensions: Length 25.4 µm, width 4.4 µm. **References:** Luthfi et al. (2024), page 12, Figure 7. **Comments:** *Catenula* sp. identified as *Catenula decusa*

Catenula sp. 1 (Figures 3.AA-3.AC). **Dimensions:** length 22.1-24.3 µm, width 4.2-4.3 µm. **References:** Luthfi et al. (2024), page 6, Figure 2. **Comments:** *Catenula* sp. 1 identified as *Paracatenula porostriata*.

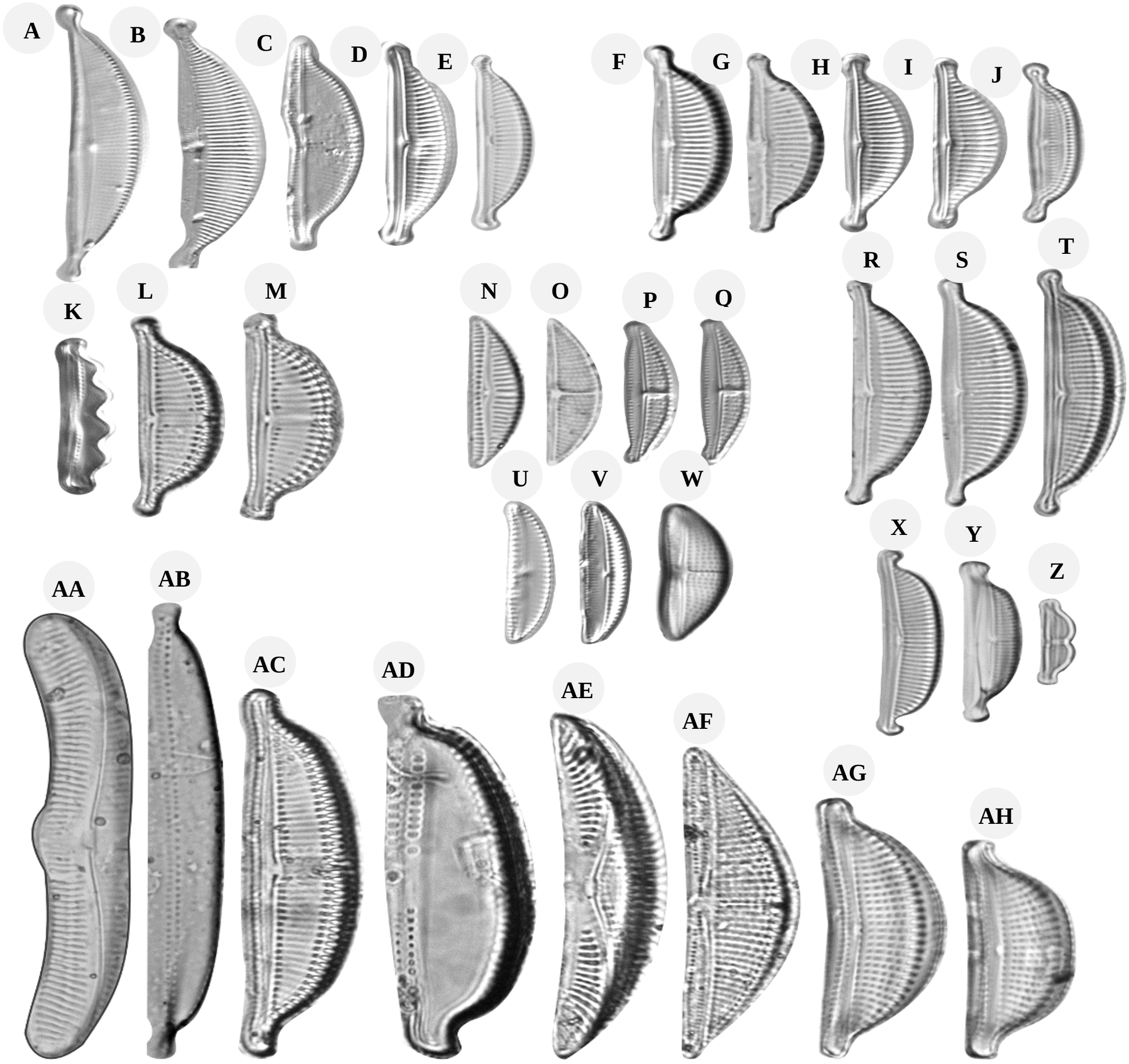

Figure 9. A-E. *Halamphora coffeiformis*; F-I. *Halamphora holsatica*; J. *Amphora* sp. 2; K. *Amphora* sp. nov; L, M, AC. *Halamphora interupta*; N. *Seminavis strigosa*; O. *Amphora montgomelyi*; P, Q. *Amphora amoena*; R-T. *Halamphora holsatica*; U. *Amphora* sp. 3; V. *Amphora* sp. 4; W. *Amphora montgomelyi*; X. *Amphora* sp. 6; Y. *Amphora* sp. 7; Z. *Halamphora kolbei*; AA. *Amphora* sp. 5; AB. *Amphora egregia* var. *interupta*; AD. *Amphora* sp. 9; A. *Amphora marina*; AF. *Amphora ostrearia*; AG, AH. *Amphora* sp. 10. Scale bar: 10 µm. LM: x1500

Catenula sp. 2 (Figure 3.AJ). **Dimensions:** Length 17 µm, width 3.2 µm. **References:** Luthfi et al. (2024), page 9, Figure 4. **Comments:** *Catenula* sp. 2 identified as *Catenula boyanensis*.

Catenula sp. 3 (Figures 3.AL-3.AN). **Dimensions:** Length 9.1-13.2 µm, width 1.9-2.6 µm. **References:** Luthfi et al. (2024), page 14, Figure 8. **Comments:** *Catenula* sp. 3 identified as *Catenula densestriata*.

Catenulopsis catenulafalsa Kryk & Witkowski (Figure 3.AK). **References:** Kryk et al. (2021), page 5, Figures 2-35. **Dimensions:** Length 13.9 µm, width 3.4 µm.

Seminavis strigosa (Hustedt) Danieledis & Economou-Amilli, 2003 (Figure 10.N). **References:** Witkowski et al. (2000), pages 770-771, pl. 164, Figures 1-4; pages 774-775, pl. 166, Figures 5-7; Danielidis and Mann (2003), page 30, Figures 23-26. **Dimensions:** Length 21.1 µm, width 5.3 µm, dorsal striae 14 in 10 µm.

Taxonomic composition

A total number of 1,619 specimens representing 139 taxa and 50 genera of coral reef diatom from Bawean Island were found. The abundance pattern of diatom taxa from numerous species to scarce is shown in Figure 15. The difference pattern species abundance smooth gradually from the highest, *D. crabro* (53 individuals), to the lowest one, *N. kariana* var. *frigida*, *G. marina* var. *undata*, *A. disculoides*, *P. campechianum*, and *C. stauroneiformis* (1 individual respectively). The relative abundance data shows that *D. crabro* is the most prevalent taxon, making up 3.3% of the sample. *P. marina* and *T. aspera* follow closely, with relative abundances of 3% (Table 2). In contrast, taxa with the lowest relative abundance include species such as *Navicula* sp. and *Achnanthes* sp., each contributing less than 0.1% to the total diatom population.

Diatom diversity and community structures

Comparing the diversity index (H') across the stations reveals no notable differences in species diversity. The southern part has the highest diversity index at 3.88, while the eastern site shows the lowest diversity at 2.64 (Table 1). The previous exhibits the lowest dominance index (0.03); on the other hand, the latter has the highest dominance index at 0.09. Evenness values across all sites are relatively high (E = 0.91), indicating a fairly even distribution of individuals among species. The diversity at each station showed a significant difference, with a p-value of 0.03, indicating that there is a statistically significant difference in species diversity among these stations (Table 1).

Table 1. Localities of study and their GPS coordinates, slide accession number, structure communities, diversity indices by station, and p-value

Site	Location	Habitat	Coordinate	Sample date	Code Repository	H'	C	E	H'*p-value*
Station 1	Gili Iyang Harbour	Rubble	5°51'11.70"S; 112°38'51.10"E	07-Jan-21	SZCZ_27552	3.34	0.05	0.91	0.03
Station 2	Mangrove Hijau Daun	Rubble	5°50'57.5"S; 112°43'3.6"E	07-Jan-21	SZCZ_27554	2.55	0.09	0.9	
Station 3	Mombhul	Rubble	5°47'21.10"S; 112°44'32.30"E	07-Jan-21	SZCZ_27555	2.84	0.07	0.91	
Station 4	Selayar Beach	Rubble	5°51'21.40"S; 112°40'59.60"E	07-Jan-21	SZCZ_27560	3.88	0.03	0.91	

Note: H': Diversity Index Shannon-Wiener; C: Dominance Index; E: Evenness Index; p-value≤0.05

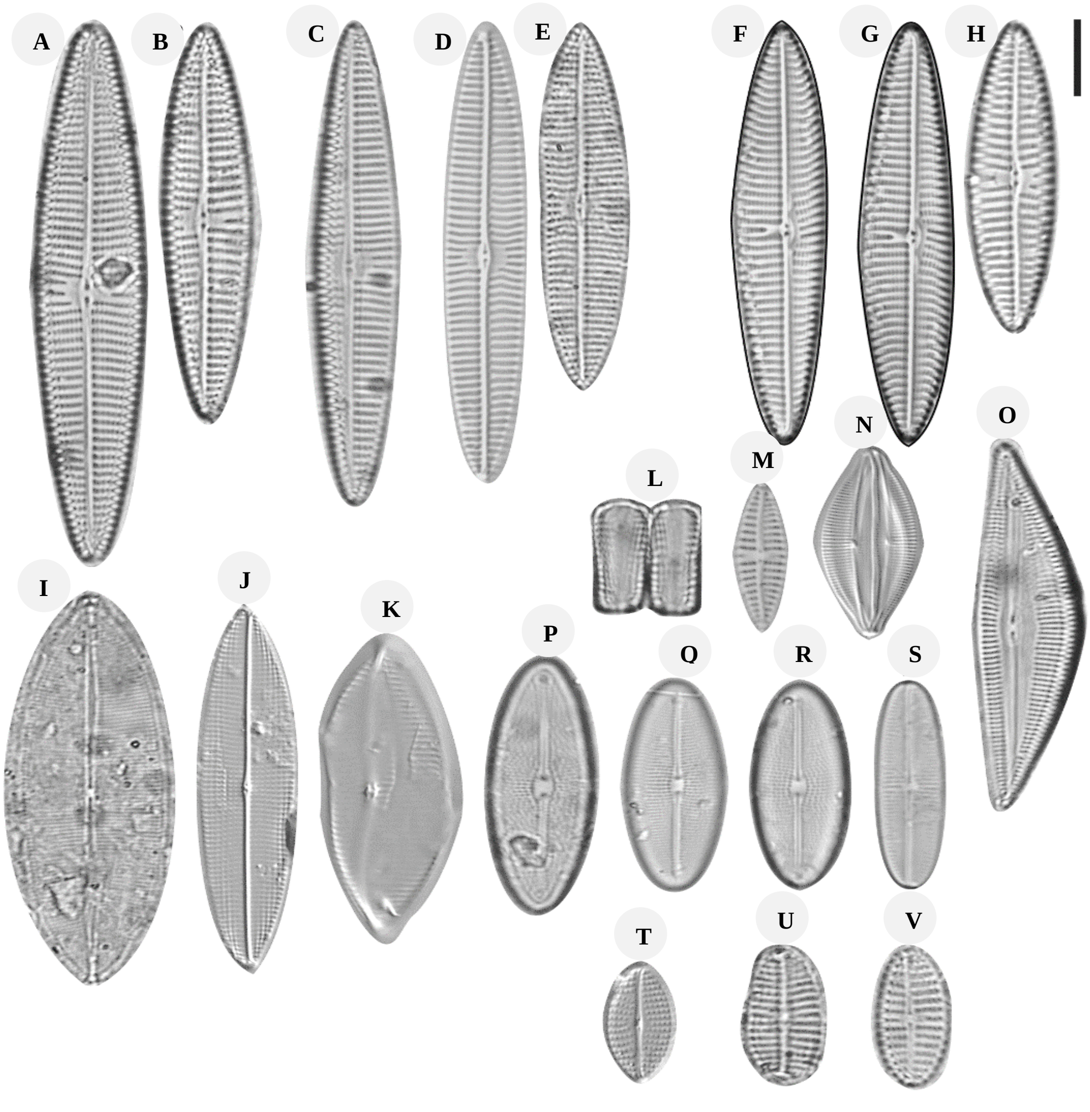

Figure 10. A, B. *Navicula directa*; C. *Navicula* sp. 1; D, E. *Navicula* sp. 2; F-H. *Navicula mollis*; I. *Navicula kariana* var. *frigida*; J. *Haslea nautica*; K. *Navicula carinifera*; L, M. *Hippodonta* sp.; N. *Halamphora coffeiformis*; O. *Seminavis robusta*; P-R. *Parlibelus delognei*; S. *Lunella* sp.; T. *Navicula* (cf.) *viminoides*; U. *Navicula* sp. 3; V. *Navicula athenea*. Scale bar: 10 µm. LM: x1500

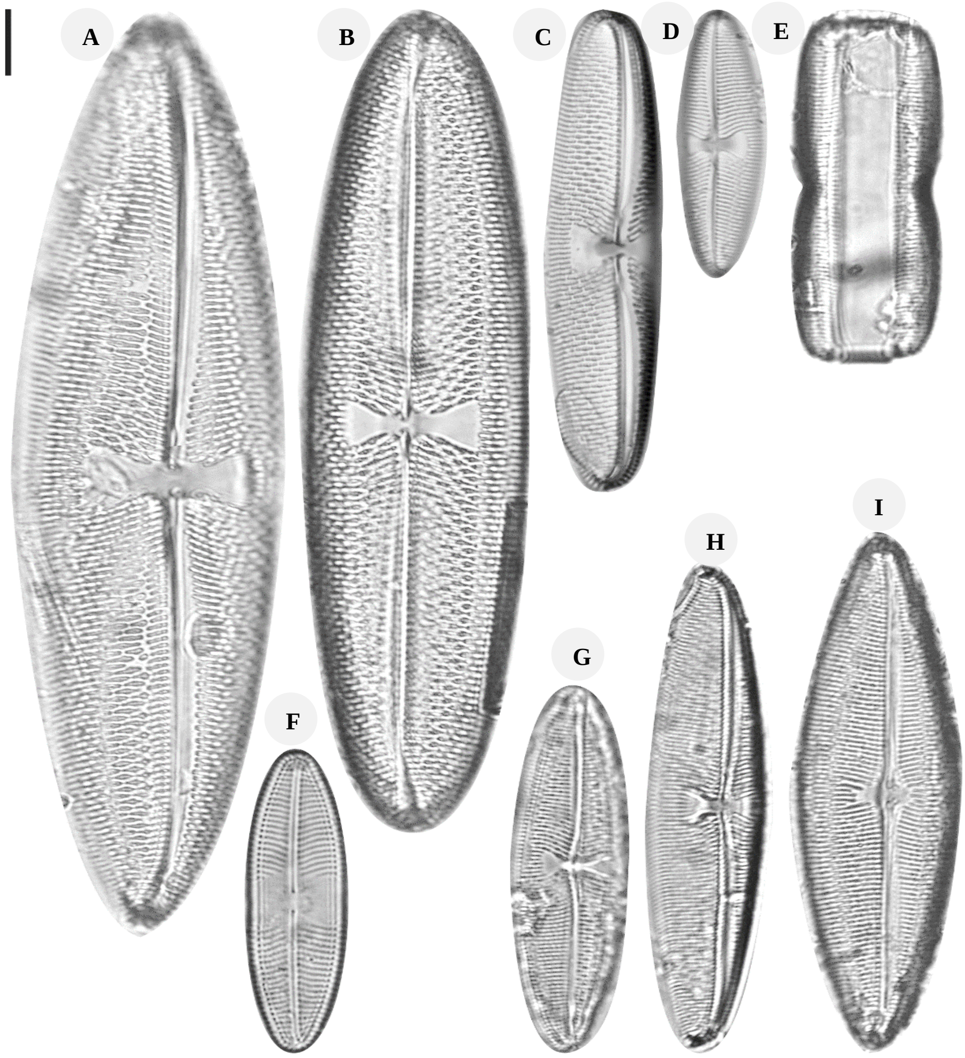

Figure 11. A-D. *Trachyneis aspera*; E. *Trachyneis aspera* girdle view; F. *Sellaphora* sp.; G-I. *Trachyneis velata*. Scale bar: 10 µm. LM: x1500

Discussion

Identified number of genera and species

The diatom flora of Bawean Island, as revealed in this research, comprises 139 taxa from 50 genera. When compared to other regions in Indonesia, the number of taxa on Bawean Island is relatively similar to each other. For instance, the South Coast of East Java hosted 365 taxa from 96 genera, while the North Coast of East Java has 156 taxa from 56 genera. The East Coast of East Java records 77 taxa from 49 genera. In contrast, West Borneo exhibits a significantly higher diversity, with 458 taxa from 131 genera. Similarly, Southeast Celebes and Southwest Celebes show considerable diversity, with 390 taxa from 91 genera and 407 taxa from 114 genera, respectively (Risjani et al. 2021). When extending this comparison to regions in the Pacific, such as Guam and Micronesia, Bawean Island's diatom diversity remains notable. Guam hosts 273 taxa from 88 genera, while Micronesia has 148 taxa from 49 genera (Lobban et al. 2012; Park et al. 2018).

The high diatom taxa richness observed on Bawean Island presents an intriguing contrast to ecosystems examined in prior research, particularly given its focus on a single habitat type: coral rubble. This finding challenges the conventional understanding that habitat diversity correlates positively with species diversity (Taxböck et al. 2020). For instance, Risjani et al. (2021) sampled diatoms from nine distinct habitats, yet only 4.7% (43 taxa) were found in dead coral (rubble). Similarly, Park et al. (2018) investigated four different macroalgal habitats (*Halimeda*, *Padina*, *Sargassum*, and *Dictyota*), while Lobban et al. (2012) collected samples from various substrates in coral reef areas. The exceptional diversity found in Bawean's coral rubble habitat suggests that this substrate may offer unique microenvironments or niche opportunities for diatoms. The complicated three-dimensional structure of coral rubble, which may offer a wide range of microhabitats, or particular chemical or physical characteristics of the degrading coral skeleton that could favor diatom colonization and diversification, could be several elements contributing to this phenomenon (Bergey et al. 2009; Wolfe et al. 2023). The findings of this study are significant because they question traditional ideas about habitat diversity and offer new ways to understand how coral rubble affects diatom diversity.

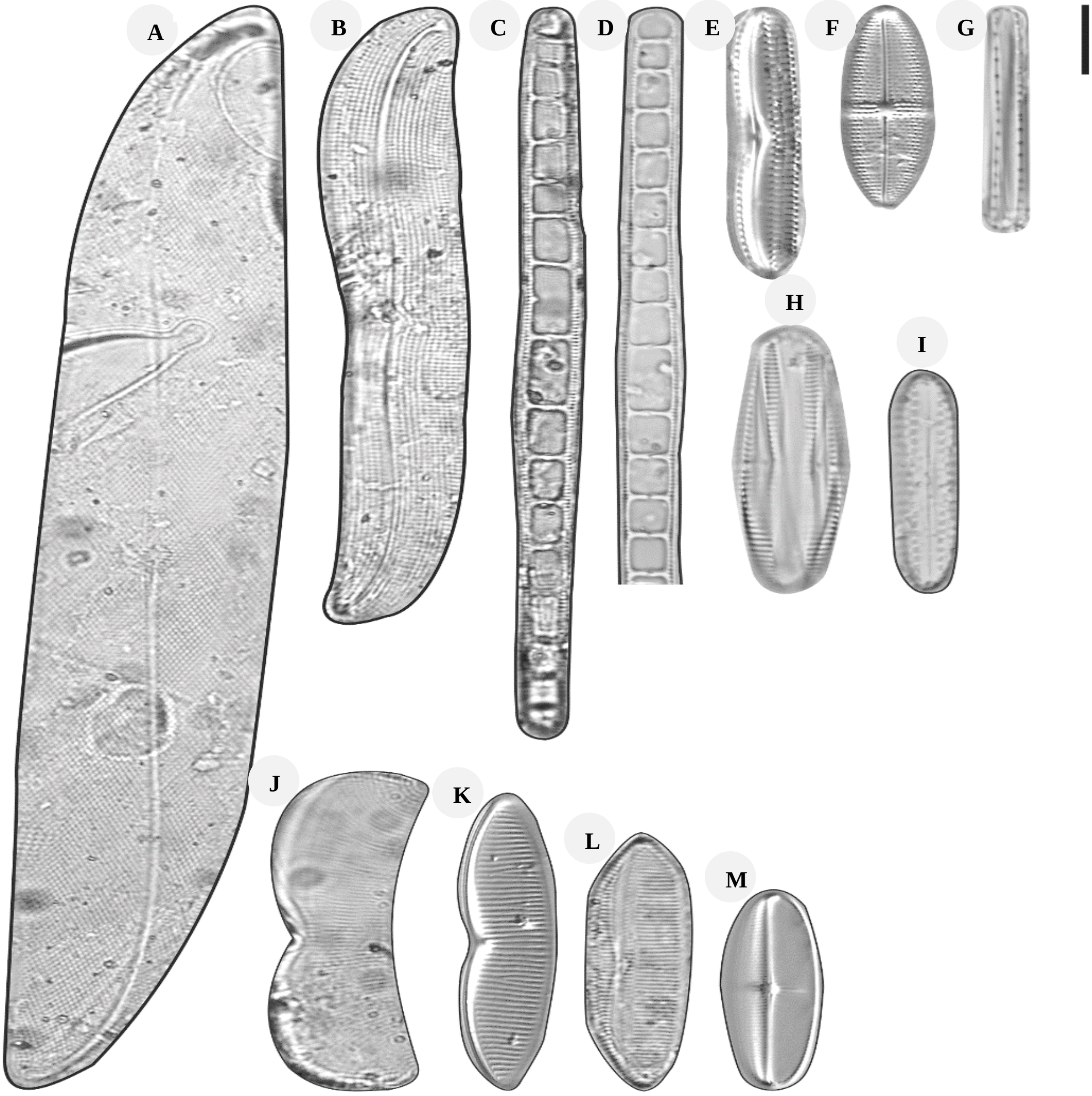

Figure 12. A. *Pleurosigma* sp.; B. *Gyrosigma* cf. *plagiostomum*; C, D. *Climaconeis lorenzii*; E, I. *Biremis ambigua*; F. *Parlibellus* sp; G. *Nitzschia distans* GV; H. *Seminavis strigosa*; I. *Pinnularia* sp; J. *Auricula intermedia*; K. *Plagiotropis* sp. 1; L. *Plagiotropis* sp. 2; M. *Parlibellus* sp. Scale bar: 10 µm. LM: x1500

Biodiversity

All four stations on Bawean Island show an evenness index of 0.9. This high and consistent value across all stations suggests a highly even distribution of species abundance across the diatom community; no single species of diatom is disproportionately abundant compared to the others. Two reasons might be addressed for this condition: first, imply similar environmental conditions across the sampling sites, i.e., coral rubble, and second, the diatom community is well-adapted to any environmental conditions that do exist (Lobo et al. 1995). The diversity of diatoms between different stations on Bawean Island was significantly different, with a p-value of 0.03. In our study, southern part of island exhibited the highest diversity with a Shannon-Wiener Index (H') of 3.88 (station 4), followed by Station 1 with an H' of 3.34. The index for diatoms indicates moderate diversity compared to nearby regions. This range falls between the diversity levels reported for various coastal areas of East Java and is generally lower than that observed in West Borneo. Specifically, the East coast of East Java exhibited an H' of 3.99, while the North and South coasts showed H' values of 3.83 and 3.6, respectively. In contrast, West Borneo demonstrated a notably higher diatom diversity with an H' of 4.22 (Risjani et al. 2021). The intermediate diversity observed on Bawean Island may be attributed to its unique geographical position between Kalimantan (Borneo) and Java, potentially reflecting a blend of environmental conditions characteristic of both larger islands.

Interestingly, this moderate diversity is notable when compared to other volcanic islands and broader regional studies. For example, the diatom community at Nosy Be Island (sample site NB10G) in the western Indian Ocean demonstrated a higher diversity with H' = 4.2 (Kryk et al. 2020). However, Bawean's diversity aligns more closely with the ranges reported for larger geographical areas.

Specifically, Redzuan et al. (2023) documented H' values spanning from 1.0 to 2.6 in the Southern China Sea, part of the Malaysian peninsula, which is higher in Pinang Island at 2.93 to 3.25 (Salleh et al. 2023). In comparison, An et al. (2018) reported a range of 4.6 to 6.1 for the Indo-western Pacific region in the tidal flats of Guenso Bay on the west coast of Korea.

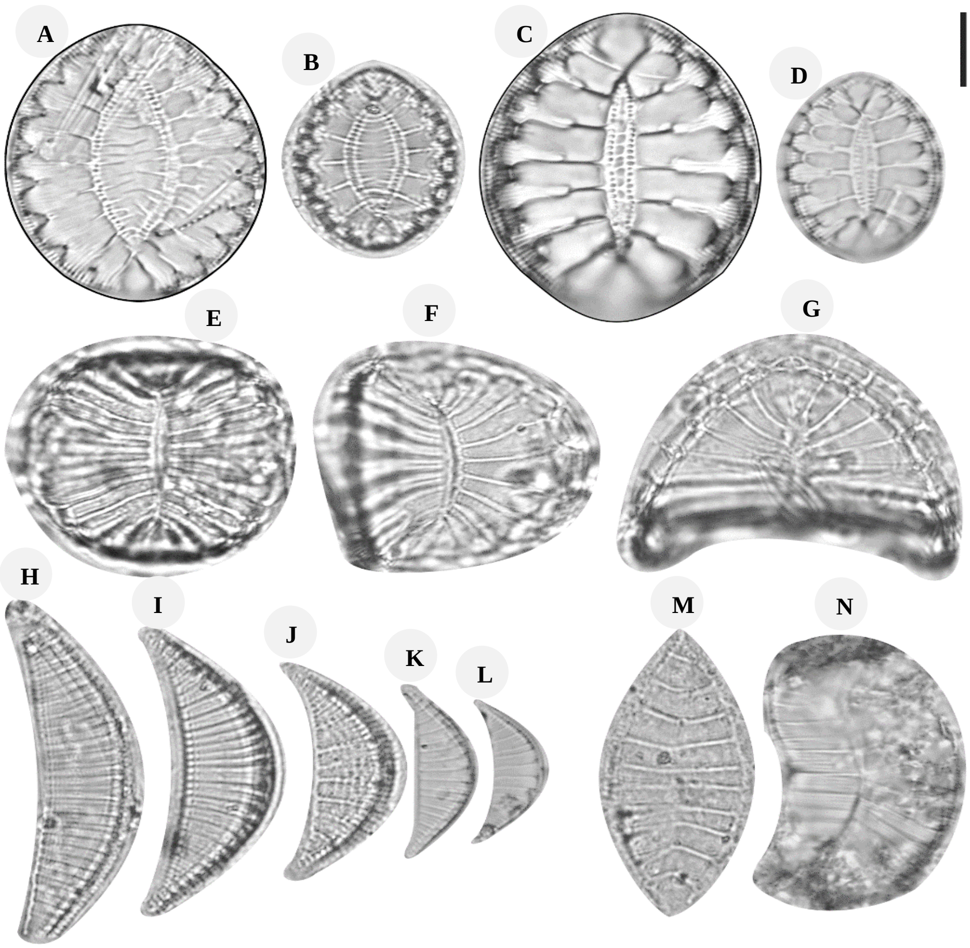

Figure 13. A-D. *Campylodiscus neofastuosus*; E-G. *Coronia decora*; H-I. *Epithemia gibberula* var. *baltica*; J. *Epithemia gracilis*; K-L. *Epithemia guettingeri*; M. *Petrodictyon gemma*; N. *Plagiodiscus nervatus*. Scale bar: 10 µm. LM: x1500

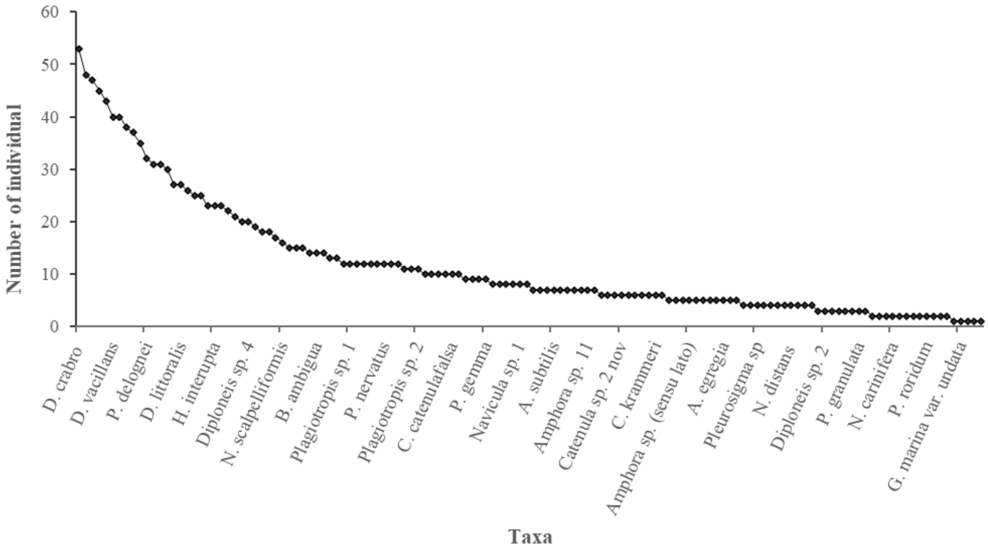

Figure 14. Equitability number of identified individuals in dominated taxa on Bawean Island, Indonesia

Table 2. List of taxa with exceeding 1% of Relative Abundance (RA)

Taxa	RA (%)
Diploneis crabro	3.3
Trachyneis aspera	3.0
Halamphora coffeiformis	2.9
Petroneis marina	2.8
Lyrella abrupta	2.7
Diploneis vacillans	2.5
Coronia decora	2.5
Psammodictyon panduriforme	2.4
Paralia sulcata	2.3
Trachyneis velata	2.2
Parlibellus delognei	2.0
Halamphora holsatica	1.9
Diploneis smithii	1.9
Diploneis notabilis	1.9
Diploneis littoralis	1.7
Cocconeis guttata	1.7
Catenula sp. 1	1.6
Diploneis cf. *mediterranea*	1.6
Nitzschia filiformis	1.6
Thalassiosira sp.	1.4
Halamphora interupta	1.4
Catenula javanica	1.4
Auricula intermedia	1.4
Psammodiscus nitidus	1.3
Lyrella sp.	1.3
Diploneis sp. 4	1.3
Seminavis strigosa	1.2
Pseudictyota dubium	1.1
Catenula sp. 3	1.1
Petroneis cf. *glacialis*	1.1

In this study, we observed that two species exhibited significant dominance on Bawean Island, with Relative Abundance (RA) of 3% (*T. aspera*) and 3.3% (*D. crabro*). Additionally, we identified four other species with RA values equal to or greater than 2.5%, which included *H. coffeiformis*, *P. marina*, *L. abrupta*, *D. vacillans*, and *C. decora*. The genus *Diploneis* is widely recognized for its prevalence in coral reef ecosystems across the Pacific region, often coexisting with various other diatom species. In Guam, a significant study by Lobban et al. (2012) documented three dominant diatom genera, including *Mastogloia*, *Cocconeis*, and *Diploneis*. Further research has corroborated these observations in other parts of the Pacific. For instance, studies conducted in the Great Barrier Reef have reported *Diploneis* frequently occurring alongside other genera such as *Amphora*, *Nitzschia*, and *Navicula* (Gottschalk et al. 2007). These findings are substantiated by research conducted in the Great Barrier Reef, where Gottschalk et al. (2007) observed *Diploneis* frequently occurring alongside five other genera: *Mastogloia*, *Cocconeis*, *Amphora*, *Nitzschia*, and *Navicula*. This consistent co-occurrence pattern suggests a potential ecological relationship or similar habitat preferences among these diatom genera. Additional evidence of *Diploneis'* extensive distribution emerges from studies across the Western Pacific, including Indonesia, Guam, and Palau, as well as Japan (Sato et al. 1983; Pennesi et al. 2017). These geographically diverse observations underscore the genus's broad ecological niche. *Diploneis* can live in many different marine environments, from warm tropical waters to cooler temperate ones. It can also grow on various surfaces and at different depths, showing how resilient this genus is. This wide-ranging distribution led Risjani et al. (2021) to classify *Diploneis* as a cosmopolitan genus.

Diploneis is recognized for its ability to thrive in diverse ecological settings, encompassing both freshwater and marine environments. This diatom genus exhibits a wide range of distribution across several aquatic environments, hence demonstrating its remarkable flexibility and persistence (Lange-Bertalot and Fuhrmann 2016). The genetic variability observed in *Diploneis* populations is subject to the influence of diverse environmental conditions, including pH, temperature, and water quality. These factors have the potential to affect the relative abundance of distinct species within the population (Pumas et al. 2018). In particular, *Diploneis* species demonstrate a highly complex valve system, which is commonly acknowledged as one of the most extensive among pennate diatom taxa. The morphology of valves imparts distinct microhabitats that facilitate the establishment and proliferation of diatoms, hence establishing an influence on the makeup of communities inside coral rubble habitats (Idei et al. 2018; Wolfe et al. 2023).

The findings suggest that coral rubble provides unique microhabitats conducive to diatom diversity, challenging the conventional understanding that habitat diversity correlates positively with species diversity. The study also compares Bawean Island's diatom diversity with other regions, noting its intermediate diversity level, which may be influenced by its geographical position between Kalimantan and Java. The presence of dominant species like *D. crabro, P. marina*, *H. coffeiformis,* and *T. aspera* underscores the ecological significance of these diatoms in coral reef ecosystems.

ACKNOWLEDGEMENTS

We would like to express our sincere gratitude to the anonymous reviewers for their thoughtful comments and constructive suggestions. This research was partially supported by the International Society for Diatom Research through the Luc Ector Early Career Award 2023. We gratefully acknowledge the financial support provided to this publication by the Polish Ministry of Science under the Regional Excellence Initiative Program for 2024-2027 (RID/SP/0045/2024/01). This work is dedicated to the memory of Professor Andrzej Witkowski, a distinguished researcher, diatomist, and mentor who passed away on 17 September 2023. Professor Witkowski's pioneering research on diatoms has significantly advanced our knowledge of these microscopic organisms.

REFERENCES

Al-Handal AY, Compère P, Riaux-Gobin C. 2016. Marine benthic diatoms in the coral reefs of Reunion and Rodrigues Islands, West Indian Ocean. Micronesica 3: 1-78. DOI: 10.5281/zenodo.13282811.

Al-Handal AY, Thomas EW, Pennesi C. 2018. Marine benthic diatoms in the newly discovered coral reefs, off Basra coast, Southern Iraq. Phytotaxa 372 (2): 111-152. DOI: 10.11646/phytotaxa.372.2.1.

Álvarez-Blanco I, Blanco S. 2014. Benthic Diatoms from Mediterranean Coasts. Schweizerbart'sche Verlagsbuchhandlung, Stuttgart, Germany.

An SM, Choi DH, Lee H, Lee JH, Noh JH, An SM, Choi DH, Lee H, Lee JH, Noh JH. 2018. Next-generation sequencing reveals the diversity of benthic diatoms in tidal flats. Algae 33 (2): 167-180. DOI: 10.4490/algae.2018.33.4.3.

Beltrones DAS, López-Fuerte FO, Martínez YJ, del Carmen Altamirano-Cerecedo M. 2021. A first estimate of species diversity for benthic diatom assemblages from the Revillagigedo Archipelago, México. Diversity 13 (10): 458. DOI: 10.3390/d13100458.

Beltrones DAS, Martínez YJ, López-Fuerte FO. 2023. Epiphytic diatoms from the central region of the Gulf of California: Floristics and biogeographic remarks. Diversity 15: 510. DOI: 10.3390/d15040510.

Bergey EA, Cooper JT, Phillips BC. 2009. Substrate characteristics affect colonization by the bloom-forming diatom *Didymosphenia geminata*. Aquat Ecol 44: 33-40. DOI: 10.1007/s10452-009-9247-6.

Car A, Witkowski A, Jasprica N, Ljubimir S, Čalić M, Dobosz S, Dupčić Radić I, Hrustić E. 2019. Epilithic diatom communities from areas of invasive Caulerpa species (*Caulerpa taxifolia* and *Caulerpa cylindracea*) in the Adriatic Sea, NE Mediterranean. Mediterr Mar Sci 20 (1): 151-173. DOI: 10.12681/mms.14330.

Claudino-Sales V, Wang P, Vasconcelos FP, Silveira AP. 2019. Environmental problems and coastal mitigation in South America: Examples from Northeast Brazil and Northern Colombia. In: Pan J, Devlin A (eds). Estuaries and Coastal Zones-Dynamics and Response to Environmental Changes. IntechOpen, London, UK. DOI: 10.5772/intechopen.87959.

Cleve PT. 1894. Kongliga Svenska Vetenskaps-Akademiens Handlingar. P.A. Norstedt & Söner, Stockholm, Sweden.

Danielidis DB, Mann DG. 2002. The systematics of *Seminavis* (Bacillariophyta): The lost identities of *Amphora angusta*, *A. ventricosa* and *A. macilenta*. Eur J Phycol 37 (3): 429-448. DOI: 10.1017/S0967026202003724.

Danielidis DB, Mann DG. 2003. New species and new combinations in the genus *Seminavis* (Bacillariophyta). Diatom Res 18 (1): 21-39. DOI: 10.1080/0269249X.2003.9705570.

De Stefano M, Marino D. 2003. Morphology and taxonomy of *Amphicocconeis* gen. nov. (Achnanthales, Bacillariophyceae, Bacillariophyta) with considerations on its relationship to other monoraphid diatom genera. Eur J Phycol 38 (4): 361-370. DOI: 10.1080/09670260310001612646.

Done T. 2011. Corals: Environmental controls on growth. In: Hopley D (eds). Encyclopedia of Modern Coral Reefs. Encyclopedia of Earth Sciences Series. Springer, Dordrecht. DOI: 10.1007/978-90-481-2639-2_10.

Droop SJM. 1998. *Diploneis sejuncta* (Bacillariophyta) and some new species from an ancient lineage. Phycologia 37 (5): 340-356. DOI: 10.2216/i0031-8884-37-5-340.1.

Foged N. 1975. Some Littoral Diatoms from the Coast of Tanzania. J. Cramer, Vaduz, Liechtenstein, German.

Giffen MH. 1975. An account of the littoral diatoms from Langebaan, Saldanha Bay, Cape Province, South Africa. Bot Mar 18 (2): 71-96. DOI: 10.1515/botm.1975.18.2.71.

Glynn PW, Enochs IC. 2010. Invertebrates and their roles in coral reef ecosystems. In: Dubinsky Z, Stambler N (eds). Coral Reefs: An Ecosystem in Transition. Springer, Dordrecht. DOI: 10.1007/978-94-007-0114-4_18.

Gottschalk S, Uthicke S, Heimann K. 2007. Benthic diatom community composition in three regions of the Great Barrier Reef, Australia. Coral reefs 26: 345-357. DOI: 10.1007/s00338-007-0204-3.

Hasle GR, Fryxell GA. 1970. Diatoms: Cleaning and mounting for light and electron microscopy. Trans Am Microsc Soc 89 (4): 469-474. DOI: 10.2307/3224555.

Idei M, Sato S, Tamotsu N, Mann DG. 2018. Valve Morphogenesis in *Diploneis smithii* (Bacillariophyta). J Phycol 54 (2): 171-186. DOI: 10.1111/jpy.12616.

John J. 2016. Diatoms from Stradbroke and Fraser Islands, Australia: Taxonomy and biogeography. Diatom Flora of Australia Vol. 1. Koeltz Botanical Books, Schmitten, Germany.

Kemp K-D, Paddock TBB. 1990. *Diademoides* nom. nov., a new generic name for *Diadema* Kemp & Paddock. Diatom Res 5 (1): 199. DOI: 10.1080/0269249X.1990.9705106.

Krammer K, Lange-Bertalot H. 1988. Bacillariophyceae 2 Teil: Bacillaricaceae, Epithemiaceae, Surirellaceae. In: Ettl H, Gerloff J, Heynig H, and Mollenhauer D (eds). Susswasserflora von Mitteleuropa. Spektrum Akademischer Verlag Heidelberg, German.

Kryk A, Bąk M, Górecka E, Riaux-Gobin C, Bemiasa J, Bemanaja E, Li C, DA̧Bek P, Witkowski A. 2020. Marine diatom assemblages of the Nosy Be Island coasts, NW Madagascar: Species composition and biodiversity using molecular and morphological taxonomy. Syst Biodivers 18 (2): 161-180. DOI: 10.1080/14772000.2019.1696420.

Kryk A, Witkowski A, Ribeiro L, Kociolek JP, Mayama S, Wróbel RJ, Risjani Y, Yunianta, Bemiasa J, Bemanaja E. 2021. Novel Diatoms (Bacillariophyta) from tropical and temperate marine littoral habitats with the description of *Catenulopsis* gen. nov., and two *Catenula* species. Diatom Res 36 (3): 265-280. DOI: 10.1080/0269249X.2021.1974572.

Kryk A. 2016. Taksonomia i bioróżnorodność zespołów okrzemkowych raf koralowych wyspy Nosy Be i północno-zachodniego Madagaskaru. [Thesis]. University of Szczecin, Poland.

Lange-Bertalot H, Fuhrmann A. 2016. Contribution to the genus *Diploneis* (Bacillariophyta): Twelve species from Holarctic freshwater habitats proposed as new to science. Fottea: J Czech Phycol Soc 16 (2): 157-183. DOI: 10.5507/fot.2015.027.

Levkov Z. 2009. Diatoms of Europe: Diatoms of the European Inland Waters and Comparable Habitats. Vol. 5. *Amphora* sensu lato: Zlatko Levkov, Gantner, Germany.

Lobban CS, Schefter M, Jordan RW, Arai Y, Sasaki A, Theriot EC, Ashworth M, Ruck EC, Pennesi C. 2012. Coral-reef diatoms (Bacillariophyta) from Guam: New records and preliminary checklist, with emphasis on epiphytic species from farmer-fish territories. Micronesica 43: 237-479.

Lobo EA, Katoh K, Aruga Y. 1995. Response of Epilithic Diatom assemblages to water pollution in rivers in the Tokyo Metropolitan area, Japan. Freshw Biol 34 (1): 191-204. DOI: 10.1111/j.1365-2427.1995.tb00435.x.

López-Fuerte FO, Beltrones DAS, del Carmen Altamirano-Cerecedo M. 2020. Species composition and new records of diatom taxa on *Phyllodictyon pulcherrimum* (Chlorophyceae) from the Gulf of California. Diversity 12 (9): 339. DOI: 10.3390/d12090339.

López-Fuerte FO, Beltrones DAS, Hernández L, Flores-Ramírez S. 2024. First account of epibiotic diatom taxa from the carapaces of green swimming crab *Callinectes bellicosus* (Stimpson 1859) (Decapoda, Portunidae). Diversity 16 (5): 302. DOI: 10.3390/d16050302.

López-Fuerte FO, Beltrones DAS, Martínez YJ, del Carmen Altamirano-Cerecedo M. 2022. Floristics and biogeographical affinity of diatoms attached to *Sargassum fluitans* (Børgesen) Børgesen and *Sargassum natans* (Linnaeus) Gaillon arriving on Mexico's Caribbean coasts. Diversity 14 (9): 758. DOI: 10.3390/d14090758.

López-Fuerte FO, Siqueiros-Beltrones DA, Navarro JN. 2010. Benthic diatoms associated with mangrove environments in the Northwest region of México. Comisión Nacional para el Conocimiento y Uso de la Biodiversidad, Universidad Autónoma de Baja California Sur, Instituto Politécnico Nacional, Centro Interdisciplinario de Ciencias Marinas, La Paz, Mexico.

Luthfi OM, Anugrah PT. 2017. Distribution of Scleractinian coral as the main reef building of coral reef ecosytem in Karang Pakiman's patch reef, Bawean Island. Depik 6 (1): 9-22. DOI: 10.13170/depik.6.1.5461. [Indonesian]

Luthfi OM, Arsad S, Kryk A, Risjani Y, Yunianta, Rybak M, Peszek Ł, Wróbel RJ, Pappas JL, Bąk M, Witkowski A. 2024. New genera and new species of Catenulaceae (Bacillariophyta) from coral reef habitat of two Indonesia islands-Bawean and Sulawesi-a morphological approach. PhytoKeys 248: 263-291. DOI: 10.3897/phytokeys.248.131839.

Luthfi OM, Priyambodo AH, Handayani M, Risjani Y, Witkowski A. 2023. Epipsammic Diatom *Cocconesis* sp. as new bioeroder in Scleractinian coral. Jurnal Ilmiah Perikanan dan Kelautan 15 (1): 162-169. DOI: 10.20473/jipk.v15i1.37653.

Madduppa H, Cahyani NKD, Anggoro AW, Subhan B, Jefri E, Sani LMI, Arafat D, Akbar N, Bengen DG. 2021. eDNA metabarcoding illuminates species diversity and composition of three phyla (Chordata, Mollusca and Echinodermata) across Indonesian coral reefs.

Biodivers Conserv 30: 3087-3114. DOI: 10.1007/s10531-021-02237-0.
Magurran AE. 1988. Ecological Diversity and Its Measurement. Croom Helm, New South Wales. DOI: 10.1007/978-94-015-7358-0.
Magurran AE. 2003. Measuring Biological Diversity. John Wiley & Sons. Oxford, United Kingdom.
Majewska R, Van de Vijver B. 2020. *Nagumoea serrata*, a new diatom species (Bacillariophyceae) found on seagrass from the south-eastern coast of Africa (Indian Ocean). Fottea 20 (1): 98-103. DOI: 10.5507/fot.2019.019.
Meister F. 1932. Kieselalgen aus Asien. Verlag von Gebrüder Borntraeger, Berlin, Germany. [Germany]
Moser G. 1998. Insel der Endemiten. Geobotanisches Phanomen Neukaledonien. Biblioth Diatomol. J. Cramer Vaduz, Liechtenstein, German. [Germany]
Navarro JN. 1981. A survey of the marine diatoms of Puerto Rico. I. Suborders Coscinodiscineae and Rhizosoleniineae. Bot Mar 24 (8): 427-440. DOI: 10.1515/botm.1981.24.8.427.
Park JS, Lobban CS, Lee K-W, Jung SW. 2022. Additional floristic study of planktonic and seaweed-associated diatoms in Chuuk, Micronesia. J Mar Biol Assoc UK 102 (1-2): 27-61. DOI: 10.1017/S002531542200025X.
Park JS, Lobban CS, Lee K-W. 2018. Diatoms associated with seaweeds from Moen Island in Chuuk lagoon, Micronesia. Phytotaxa 351 (2): 101-140. DOI: 10.11646/phytotaxa.351.2.1.
Pennesi C, Caputo A, Lobban CS, Poulin M, Totti C. 2017. Morphological discoveries in the genus *Diploneis* (Bacillariophyceae) from the tropical west Pacific, including the description of new taxa. Diatom Res 32 (2): 195-228. DOI: 10.1080/0269249X.2017.1343752.
Peragallo H, Peragallo M. 1897. Diatomées marines de France et des districts maritimes voisins. Texte, Tempère. Grez-sur-Loing, France. DOI: 10.5962/bhl.title.68918. [France]
Pielou EC. 1966. The measurement of diversity in different types of biological collections. J Theor Biol 13: 131-144. DOI: 10.1016/0022-5193(66)90013-0.
Plinski M, Witkowski A. 2020. Diatoms From the Gulf of Gdansk and Surrounding Waters (the Southern Baltic Sea). A Key to the Identification of the Species. Gdansk University Press, Gdansk, Poland.
Pumas C, Pruetiworanan S, Peerapornpisal Y. 2018. Diatom diversity in some hot springs of Northern Thailand. Botanica 24 (1): 69-86. DOI: 10.2478/botlit-2018-0007.
Redzuan NS, Abdullah MM, Norizan NA. 2023. Common genus of benthic Diatoms on the seafloor of the Southern South China Sea, Peninsular Malaysia-A preliminary survey. Univ Malays Terengganu J Undergrad Res 5 (3): 44-50. DOI: 10.46754/umtjur.v5i3.376.
Risjani Y, Witkowski A, Kryk A, Yunianta, Górecka E, Krzywda M, Safitri I, Sapar A, Dąbek P, Arsad S, Gusev E, Rudiyansyah, Peszek Ł, Wróbel RJ. 2021. Indonesian coral reef habitats reveal exceptionally high species richness and biodiversity of diatom assemblages. Estuar Coast Shelf Sci 261: 107551. DOI: 10.1016/j.ecss.2021.107551.
Ruggiero MA, Gordon DP, Orrell TM, Bailly N, Bourgoin T, Brusca RC, Cavalier-Smith T, Guiry MD, Kirk PM. 2015. A higher level classification of all living organisms. PLoS One 10 (4): e0119248. DOI: 10.1371/journal.pone.0119248.
Salleh S, Cheng EEL, Hossain MS, Samad S, Mubin NAAA, Darif NAM, Jonik MGG, Mohammad M. 2023. The photophysiology of benthic Diatoms in the intertidal flats of Pulau Pinang (Malaysia). Pertanika J Sci Technol 31 (2): 1-21. DOI: 10.47836/pjst.31.2.13.
Sato H, Maeda Y, Kumano S. 1983. Diatom assemblages and Holocene Sea level changes at the Tamatsu site in Kobe, western Japan. Quat Res (Daiyonki-Kenkyu) 22 (2): 77-90. DOI: 10.4116/jaqua.22.77.
Shannon CE. 1948. A mathematical theory of communication. Bell Syst Tech J 27 (3): 379-423. DOI: 10.1002/j.1538-7305.1948.tb01338.x.
Stidolph SR, Sterrenburg FAS, Smith KEL, Kraberg A. 2012. Stuart R. Stidolph Diatom Atlas. US Geological Survey, Reston, VA. DOI: 10.3133/ofr20121163.
Taxböck L, Karger DN, Kessler M, Spitale D, Cantonati M. 2020. Diatom species richness in Swiss springs increases with habitat complexity and elevation. Water 12 (2): 449. DOI: 10.3390/w12020449.
Wachnicka AH, Gaiser EE. 2007. Characterization of *Amphora* and *Seminavis* from south Florida, USA. Diatom Res 22 (2): 387-455. DOI: 10.1080/0269249X.2007.9705722.
Witkowski A, Lange-Bertalot H, Metzeltin D. 2000. Diatom Flora of Marine Coasts I. Iconographia Diatomol. Koeltz Botanical Books, Schmitten, Germany.
Wolfe K, Kenyon TM, Desbiens A, de la Motte K, Mumby PJ. 2023. Hierarchical drivers of Cryptic biodiversity on coral reefs. Ecol Monogr 93 (3): e1586. DOI: 10.1002/ecm.1586.
Wolfe K, Kenyon TM, Mumby PJ. 2021. The biology and ecology of coral rubble and implications for the future of coral reefs. Coral Reefs 40: 1769-1806. DOI: 10.1007/s00338-021-02185-9.